MONTHLY NOTICES

OF THE

ROYAL ASTRONOMICAL SOCIETY

Vol. 110 No. 3 1950

Published and Sold by the
ROYAL ASTRONOMICAL SOCIETY
BURLINGTON HOUSE
LONDON, W. 1

Price Nine Shillings

NOTICE TO AUTHORS

1. *Communications.*—Papers must be communicated to the Society by a Fellow. They should be accompanied by a summary at the *beginning* of the paper conveying briefly the content of the paper, and drawing attention to important new information and to the main conclusions. The summary should be intelligible in itself, without reference to the paper, to a reader with some knowledge of the subject; it should not normally exceed 200 words in length. Authors are requested to submit MSS. in duplicate. These should be typed, using double spacing and leaving a margin at one side. Corrections to the MSS. should be made in the text and not in the margin. By Council decision, MSS. of accepted papers are retained by the Society for one year after publication; unless their return is then requested by the author, they are destroyed.

2. *Presentation.*—Authors are allowed considerable latitude, but they are requested to follow the general style and arrangement of *Monthly Notices*. References to literature should be given in the standard form, including a date, for printing either as footnotes or in a numbered list at the end of the paper. Each reference should give the name of the author cited, irrespectively of the occurrence of the name in the text (some latitude being permissible, however, in the case of an author referring to his own work).

3. *Notation.*—Authors should conform closely with the recommendations of Commission 3 of the International Astronomical Union (*Trans. I.A.U.*, Vol. VI, p. 345, 1938). Council has decided to adopt the I.A.U. 4-letter abbreviations for constellations where contraction is desirable (Vol. IV, p. 221, 1932).

4. *Diagrams.*—These should be drawn about twice the size required in print and prepared for direct photographic reproduction except for the lettering which should be inserted in pencil. Legends should be given in the manuscript indicating where in the text the figure should appear. Blocks are retained by the Society for 10 years; unless the author requires them before the end of this period they are then destroyed.

5. *Tables.*—These should be arranged so that they can be printed upright on the page.

6. *Proofs.*—Costs of alteration exceeding 5 per cent of composition must be borne by the author. Fellows are warned that such costs have risen sharply in recent years, and it is in their own and the Society's interests to seek the maximum conciseness and simplification of symbols and equations consistent with clarity.

7. *Revised Manuscripts.*—When papers are submitted in revised form it is especially requested that they be accompanied by the original MS.

Reading of Papers at Meetings

8. If a paper is to be read at a meeting it should be received by the Assistant Secretary not later than the previous Friday.

9. When submitting papers authors are requested to indicate whether they will be willing and able to read the paper at the next or some subsequent meeting, and approximately how long they would like to be allotted for speaking.

10. Postcards giving the programme of each meeting are issued some days before the meetings concerned. Fellows wishing to receive such cards whether for the Ordinary Meetings or for the Geophysical Discussions or both should notify the Assistant Secretary.

MONTHLY NOTICES

OF THE

ROYAL ASTRONOMICAL SOCIETY

Vol. 110 No. 3

MEETING OF 1950 MARCH 10

Professor W. M. Smart, President, in the Chair

The election by the Council of the following Fellows was duly confirmed:—

Reginald Gordon Andrews, The Old Brick House, Town Littleworth, Cooksbridge, Lewes, Sussex (proposed by F. M. Holborn);

Henry Reginald Calvert, M.A., B.Sc., D.Phil., The Science Museum, South Kensington, S.W.7 (proposed by R. d'E. Atkinson);

Herbert Chatley, D.Sc., M.I.C.E., A.Inst.P., 4 Belgrave Road, Grosvenor, Bath (proposed by A. T. Doodson);

Arthur D. Code, Leander McCormick Observatory, University of Virginia, Charlottesville, Virginia, U.S.A. (proposed by S. Chandrasekhar);

Sidney Charles Bartholomew Gascoigne, Commonwealth Observatory, Mount Stromlo, Canberra, Australia (proposed by R. v. d. R. Woolley);

John Herbert Hewitt, 60 Farquhar Road, Edgbaston, Birmingham (proposed by M. C. Johnson);

Arthur Robert Hogg, Commonwealth Observatory, Mount Stromlo, Canberra, Australia (proposed by R. v. d. R. Woolley);

John Alexander Jenkins, Glaselune, Balerno, Midlothian, Scotland (proposed by W. M. H. Greaves);

Ralph Leslie Maughan, M.Sc., F.Inst.P., Constantine Technical College, Middlesbrough, Yorkshire (proposed by F. R. Curtis);

Alexander Charles Robbins, 64 Eastbury Road, Northwood, Middlesex (proposed by R. C. Wood); and

Leonard Stanley Theodore Symms, 21 Shrewsbury Lane, Shooter's Hill, London, S.E.18 (proposed by R. d'E. Atkinson).

One hundred and twelve presents were announced as having been received since the last meeting, including:—

Harlow Shapley, *Galactic and Extra-Galactic Studies. First Collection* (presented by the author);

Peter Doig, *A Concise History of Astronomy* (presented by the author);

Harold Jeffreys, *Earthquakes and Mountains* (presented by the author);

Gérard de Vaucouleurs, *The Planet Mars* (presented by the author); and

P. A. Schilpp, Ed., *Albert Einstein: Philosopher Scientist. Volume VII of the Library of Living Philosophers* (presented anonymously).

MEETING OF 1950 APRIL 14

Professor W. M. Smart, President, in the Chair

The election by the Council of the following Fellows was duly confirmed:—

Alan Hugh Cook, Department of Geodesy and Geophysics, Downing Place, Cambridge (proposed by B. C. Browne);

Sidney Guy Hacker, Department of Mathematics, State College of Washington, Pullman, Washington, U.S.A. (proposed by H. N. Russell);

John Meadows Jackson, B.Sc., Ph.D., University College, Dundee (proposed by Sir Edmund Whittaker);

Gerry Marlowe, The Stables, Burford Drive, Whalley Range, Manchester, 16 (proposed by J. C. Farrer); and

Stanley Keith Runcorn, Gonville and Caius College, Cambridge (proposed by R. I. B. Cooper).

One hundred and fourteen presents were announced as having been received since the last meeting, including:—

Angus Armitage, *A Century of Astronomy* (presented by the author);

Oliver Justin Lee, *Measuring our Universe* (presented by the author); and

An original photograph of Comet 1948l taken during the Eclipse (presented by R. O. Hennings).

The President announced that the Council had gratefully accepted a legacy, amounting to approximately £750, from the late Mrs M. A. Nadarov, bequeathed to the Society in the following terms:—

"To the Royal Astronomical Society, Burlington House, London, for the encouragement and promotion of the study of Sunspots, and to be known as the Victor Nadarov Fund."

A STUDY OF THE ERUPTIVE PROMINENCE OF 1948 SEPTEMBER 27

Helen W. Dodson and Edwin B. Weston

(Communicated by Robert R. McMath)

(Received 1950 March 10)

Summary

Motions in an eruptive prominence are discussed. The radial velocities of the prominence gases are found to be consistent with the cross-motions shown by the spectroheliograms. This agreement is strong evidence in favour of the hypothesis of moving material. Motions of descending nodules and of an unusual ascending spike are included in the study.

1. *Introduction*

On 1948 September 26 and 27, a large prominence was observed to arch across the solar equator on the east limb of the Sun. A unipolar spot (Mount Wilson No. 9438), with field strength 1100 gauss, was located near its northern extremity. There was no spot near the southern extremity. Throughout September 26, faint knots or streamers passed from the southern to the northern branches of the prominence. This type of activity continued until 15^h on September 27 when the entire bright southern branch of the prominence began to move upward and along the arch. As this bright mass advanced it disturbed the stability of the arch and the entire phenomenon became an eruptive prominence. Hydrogen spectroheliograms secured with the Tower Telescope of the McMath-Hulbert Observatory and spectra recorded by the Stone Spectroheliograph permit a detailed study of the prominence and provide evidence in favour of the hypothesis of moving material within the prominence. A well-defined ascending spike was a secondary feature of considerable interest.

Intercomparison of radial velocities and motions in the plane of the sky, coupled with the data secured on the two successive days, indicate that on September 27 the northern tip of the prominence extended over the disk while the southern extremity emanated from a point on or behind the limb. Motion from south to north along the arch of the prominence would thus contain a component directed towards the observer.

2. *Summary of Principal Activity*

(*a*) Between $15^h\,40^m$ and $17^h\,30^m$ the bright mass moved northward, upward and towards the observer with slowly increasing velocity.

(*b*) During this period, at least part of the bright mass was in rotation about an axis that was more nearly radial than tangential to the solar surface. As viewed from the centre of the Sun the direction of rotation was counter-clockwise. The rotation is apparent when the film is viewed as a cinema and it is confirmed by the positive and negative radial velocities in the spectra.

(*c*) As the bright mass advanced, it disturbed the relatively stable arch or streamer that had been observed since September 26. It should be noted that

prior to 17^h00^m there was no significant change in the position of the northern half of the arch even though the southern half had been completely modified.

(*d*) Between 16^h23^m and 17^h08^m there developed within the prominence a conspicuous pattern which was concave upward. As the bright mass moved, the pattern moved; its orientation was fixed with respect to the moving prominence, not with respect to the chromosphere or photosphere. Fig. 1 (Plate 3) shows this pattern at 16^h29^m and 16^h56^m.

(*e*) Material continually dropped back to the chromosphere, principally along the northern and southern branches of the original arch, but in part along new paths emanating from the bright mass. The descending material along the northern branch was more intense than that along the southern branch. This is clearly shown in the series of spectra for 17^h28^m.

(*f*) In the final stages of the activity (17^h25^m to 19^h00^m) the "bright mass" and the remnant of the stable arch completely merged. The configuration expanded, and as it rose in height it continued to feed material back to the disk. The prominence was measured to a height of 500,000 km. above the solar surface. After 18^h35^m the spectroheliograms showed only descending material.

3. *Velocities and Accelerations in Principal Activity*

Although the phenomenon was complex and many of the features ephemeral or diffuse, it was possible to measure with a certain confidence the x and y coordinates of a limited number of regions. In the system of rectangular coordinates in which the measurements were made, the origin was on the solar limb in latitude 3° south, the x-axis was tangential to the solar disk at this point, and the y-axis passed through the origin in the direction of the radius of the apparent solar disk.* The measures of x and y are plotted versus time in Fig. 2. Velocities in the x and y directions have been determined from the slopes of curves drawn through the mean of the plotted points. It should be noted that in this study the measurement of x was considerably less certain than that of y. Velocities in the z, or radial, direction have been determined from spectroheliograms taken with the Stone Spectroheliograph.† The radial velocities are based on displacements of $H\alpha$ emission of the prominence measured with respect to the dark $H\alpha$ line of the scattered light from the adjacent solar limb. The effect of solar rotation on the radial velocities is thus eliminated. The spectra in Fig. 1 (Plate 3) are oriented in such a manner that negative radial velocities are represented by displacements downward; positive radial velocities result in displacements upward. Radial velocities are not available for the highest parts of the prominence nor for the very faint portions within it. In the former case the regions were beyond the field of the Stone instrument; in the latter case the spectra were too weak for satisfactory registration.

During the period 15^h40^m to 17^h30^m the velocities in the x, y and z directions were of the same order of magnitude (10 to 30 km./sec.). The values are recorded in Table I. The magnitude and direction of the velocities in the xy-plane (the plane of the sky) are shown graphically in Fig. 3(*a*) against the background of the prominence. The tracks of the arrows in this diagram trace the trajectories of

* A more detailed description of this coordinate system is given in *Publ. Obs. Univ. Mich.*, **8**, 123, 1941.

† Detailed descriptions of the instrument and the method of measurement are given in *Publ. Obs. Univ. Mich.*, **8**, 57, 1940.

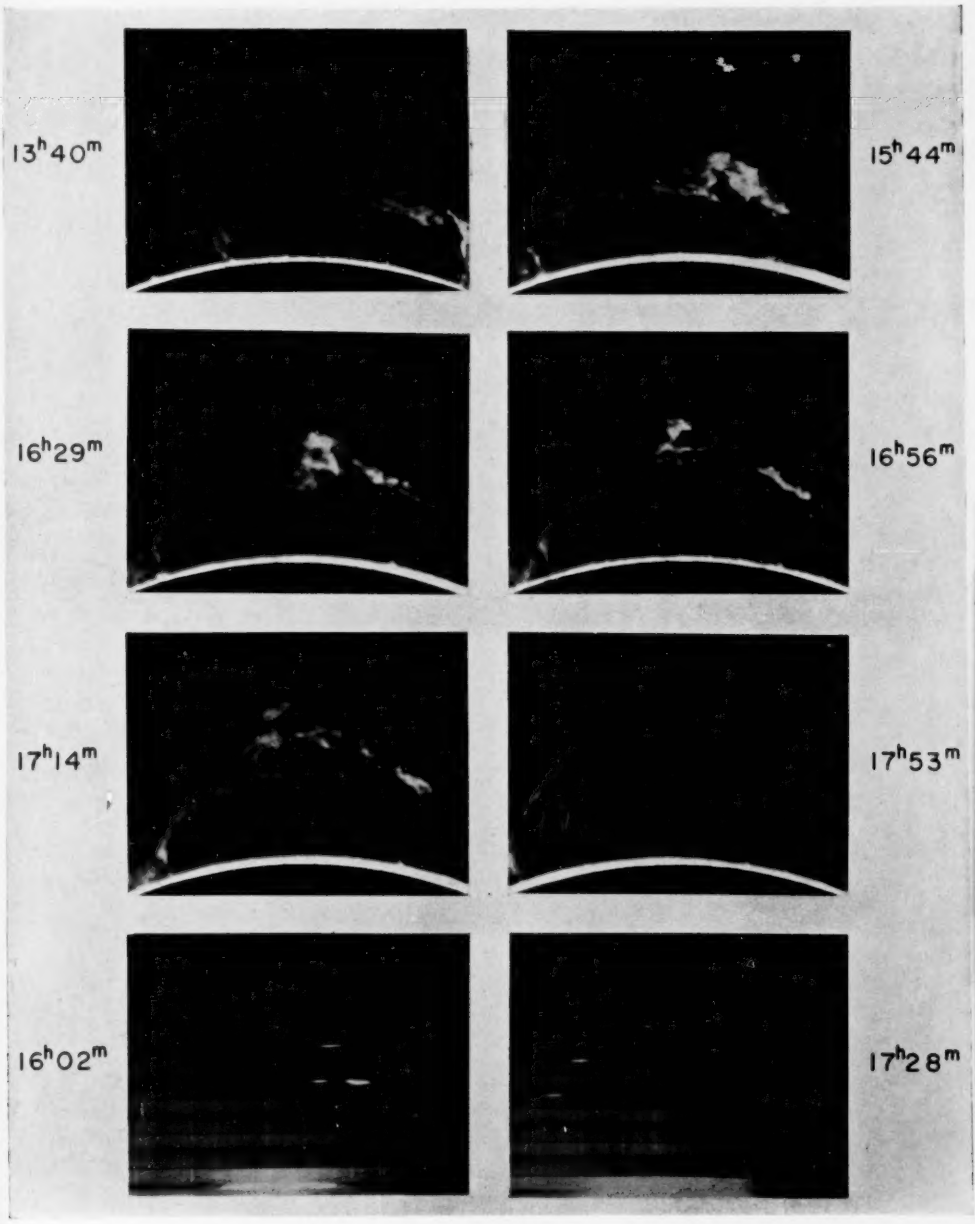

FIG. 1.—*Hα spectroheliograms and spectra for the prominence of 1948 September 27.*

the measured features. Concurrent radial velocities in km./sec. are indicated by the adjacent numbers.

Between $17^h\,30^m$ and $18^h\,30^m$, velocities in the y, or height, direction increased rapidly. For all ascending features the last measurable spectroheliograms indicate outward velocities between 150 and 200 km./sec. The similarity of the y versus time curves for the various features should be noted.

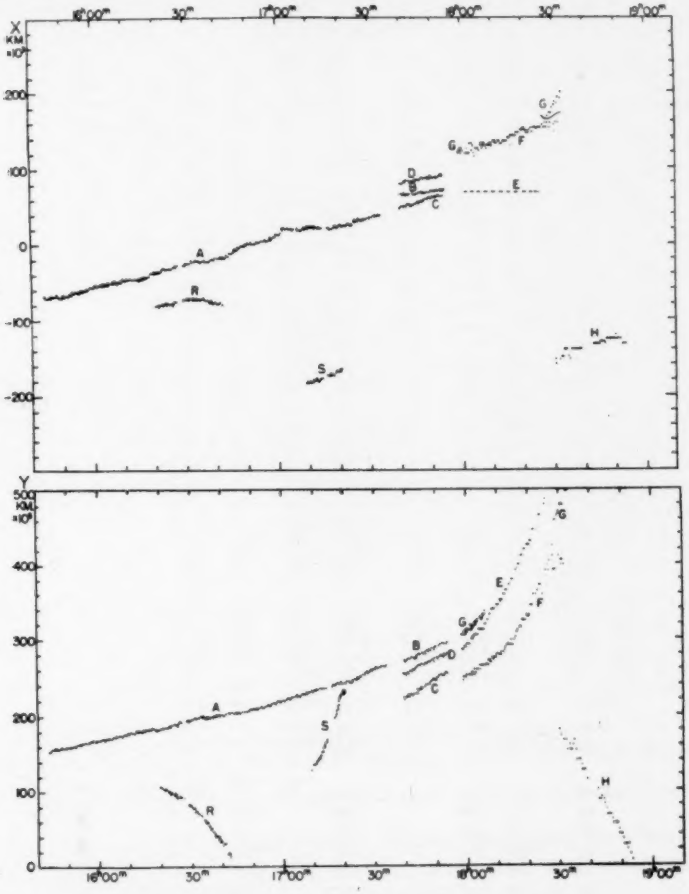

FIG. 2.—*Plot of x and y for all measured features in the prominence.*

The accelerations in the xy-plane represented by these velocities are likewise recorded in Table I and shown graphically in Fig. 3 (*b*). It should be emphasized that accelerations are measures of second differences and of necessity carry a high degree of uncertainty. There are, nevertheless, certain aspects that seem clearly indicated. Throughout the entire activity, accelerations in the x direction were small; the same is indicated by all available data for the z-plane. Accelerations in the y, or height, direction dominated the activity and these began

TABLE I

Positions, Velocities and Accelerations for the Measured Features of the Prominence of 1948 September 27

Feature measured	Time 1948 Sept. 27		Position (km. × 10^3)		Velocity (km./sec.)					Acceleration (km./sec.^{2} × 10^{-3})			
	h	m	X	Y	V_x	V_y	V_z	V_{xy}	V_{xyz}	A_x	A_y	A_z	$A_z\sqrt{A_x^2+A_y^2}$
						Principal Activity							
Top point of ascending bright mass	15	45	−70	156	14	12	−10	18	21	0·6	0·8	−2	1
		50	−66	160	14	12	−11	18	22	0·6	0·8	−2	1
		55	−62	164	15	12	−11	19	22	0·6	0·8	−2	1
	16	00	−57	168	15	13	−12	20	23	0·6	0·8	−2	1
A		05	−52	172	16	13	−12	21	24	0·6	0·8	−2	1
		10	−48	176	16	13	−13	21	24	0·6	0·8	−2	1
		15	−44	180	16	13	−14	21	25	0·6	0·8	−3	1
		20	−38	184	16	13	−15	21	26	0·6	0·8	−3	1
		25	−33	188	17	14	−15	22	27	0·6	0·8	−3	1
		30	−28	192	17	14	−16	22	27	0·6	0·8	−3	1
		35	−23	196	17	14	−17	22	28	0·6	0·8	−3	1
		40	−17	200	17	14	−18	22	29	0·6	1	−3	1
		45	−12	204	17	14	−19	22	29	0·6	2	−3	2
		50	(−8)	208	17	16	−20	23	31	0·6	2	−3	2
		55	(−2)	213	17	18	−21	25	32	0·7	3	−3	3
	17	00	(4)	219	17	19	−21	25	33	0·7	4	−3	4
		05	(8)	225	17	20	−22	26	34	0·7	4	−3	4
		10	(13)	231	17	21	−23	27	35	0·7	6	−3	6
		15	19	237	18	22	−23	28	37	0·8	7	−3	7
		20	24	244	18	23	−24	29	38	0·8	8	−3	8
		25	30	252	19	28	−25	34	42	0·8	9	−3	9
		30	36	260	20	31	−26	37	45	1·0	12	−3	12
Ascending nodules	17	40	62	276	14	42	−28	44	52		*		
B		45	65	290	14	42	−30	44	54				
		50	70	302	14	42	−40	44	60				
C	17	40	48	222	23	45	−28	50	58		*		
		45	54	234	23	45	−30	50	59				
		50	62	248	23	45	−40	50	64				
D	17	40	80	254	14	34	−28	37	46		*		
		45	84	264	14	34	−30	37	48				
		50	88	274	14	34	−40	37	54				
E	18	00	†70	292	†	72	−50	72	88	†	68	...	68
		05	70	316	...	96	...	96	...	...	68	...	...
		10	70	348	...	113	...	113	...	...	68	...	...
		15	70	384	...	141	...	141	...	...	68	...	...
		20	70	430	...	155	...	155	...	...	68	...	...
		25	70	478	...	155	...	155	...	...	68	...	...
F	18	00	116	252	22	34	−50	40	64	1	29	...	29
		02·5	120	258	22	40	...	46	...	1	40	...	40
		05	124	264	22	45	...	50	...	1	42	...	42
		07·5	128	270	22	48	...	53	...	1	55	...	55
		10	132	278	22	58	...	62	...	1	60	...	60
		12·5	135	288	22	72	...	75	...	1	82	...	82
		15	138	300	22	89	...	92	...	1	103	...	103
		17·5	142	316	22	116	...	118	...	1	144	...	144
		20	146	336	22	145	...	147	...	1	188	...	188
		22·5	150	360	22	163	...	164	...	1	210	...	210

TABLE I—*Continued*

Positions, Velocities and Accelerations for the Measured Features of the Prominence of 1948 September 27

Feature measured	Time 1948 Sept. 27		Position (km. × 10^3)		Velocity (km./sec.)						Acceleration (km./sec.^{2} × 10^{-3})		
	h	m	X	Y	V_x	V_y	V_z	V_{xy}	V_{xyz}	A_x	A_y	A_z	$A_z\sqrt{A_x^2+A_y^2}$
						Principal Activity							
Ascending nodule													
G	18	00	116	308	6	68	−50	68	85	...	65	...	(65)
		05	120	330	6	68	...	68	...	...	65	...	(65)
		...	...	...	...	...	...	...	...	...	...	...	...
		...	...	...	...	...	...	...	...	...	...	...	...
		...	...	...	...	...	...	...	...	...	...	...	...
		...	...	...	...	...	...	...	...	...	...	...	...
		30	180	470	115	180	...	214	...	...	65	...	(65)
Descending	18	30	−149	184	19	−121	86	123	150	0	0	...	0
material		35	−144	148	19	−121	‡	123	...	0	0	...	0
after		40	−138	112	19	−121	...	123	...	0	0	...	0
eruption		45	−132	74	19	−121	...	123	...	0	0	...	0
H		50	−126	38	19	−121	...	123	...	0	0	...	0
		55	−120	0	19	−121	...	123	...	0	0	...	0
						Secondary Activity							
Descending	16	20	−82	106	...	...	...	...	...	...	...	...	...
nodules		22·5	−80	100	...	...	...	...	...	...	...	...	...
ejected from		25	−77	93	21	−43	(−25)	48	(54)	−25	−66	...	70
ascending		27·5	−74	86	17	−51	(−25)	54	(59)	−32	−66	...	73
bright mass		30	−72	80	13	−59	(−25)	60	(65)	−45	−66	...	80
R		32·5	−72	70	2	−73	(−25)	72	(76)	−75	−66	...	100
		35	−73	58	−9	−86	(−25)	86	(90)	−68	−66	...	95
		37·5	−75	42	−16	−94	(−25)	95	(99)	−37	−66	...	76
		40	−78	30	−17	−104	(−25)	104	(107)	−28	−66	...	72
		42·5	−82	10	−24	−112	(−25)	115	(117)	−21	−66	...	69
Ascending	17	10	−183	134	14	116	−46	117	125	58	189	−30	198
spike		12·5	−180	150	21	154	−51	156	163	58	189	−30	198
S		15	−176	174	30	198	−56	201	208	58	189	−30	198
		17·5	−172	208	34	201	−61	204	213	58	189	−30	198
		20	−168	238	50	198	−64	204	214	58	189	−30	198

( ) Uncertain value.

* Measures cover too short a time interval for determination of acceleration.

† No significant change in the value of X, but measures are too uncertain to permit meaningful determinations of velocity and acceleration.

‡ The radial velocity for this object is positive but its change in value with time is unknown.

to increase in magnitude at about $17^h\,00^m$. Within the range of the measurements the accelerations in the y direction either remained constant or increased with increasing height.

After $18^h\,30^m$, the principal feature was a relatively bright descending nodule (Feature H). This appeared to move in the xy-plane with the large constant velocity of 123 km./sec. Its radial velocity at $18^h\,30^m$ was +86 km./sec.

4. *Secondary Activity*

(1) ***Descending nodules ejected from ascending bright mass.***—At about $16^h\,15^m$ a series of knots (Feature R) was ejected from one of the rotating "veins" of the ascending mass. As the knots descended they formed a streamer and

entered the chromosphere near latitude 10° south. The individual knots followed curved trajectories in the *xy*-plane, but their locus at any one instant was essentially linear. The feature is clearly shown in the spectroheliogram for $16^h 29^m$ in Fig. 1. At $16^h 15^m$ the point from which the nodules emanated showed the presence of gases with radial velocities of the order of -80 km./sec. It is not possible to determine the variation of V_z with time for the individual nodules, but the data are sufficient to show that the radial velocities remained negative and between $16^h 25^m$ and $16^h 45^m$ were of the order of -25 km./sec.

The x and y measures for the first knot ejected are shown as Feature (R) in Table I and Figs. 2 and 3. The velocities increased with time and the space accelerations showed a relatively larger component at right angles to the trajectory than was the case for the ascending material.

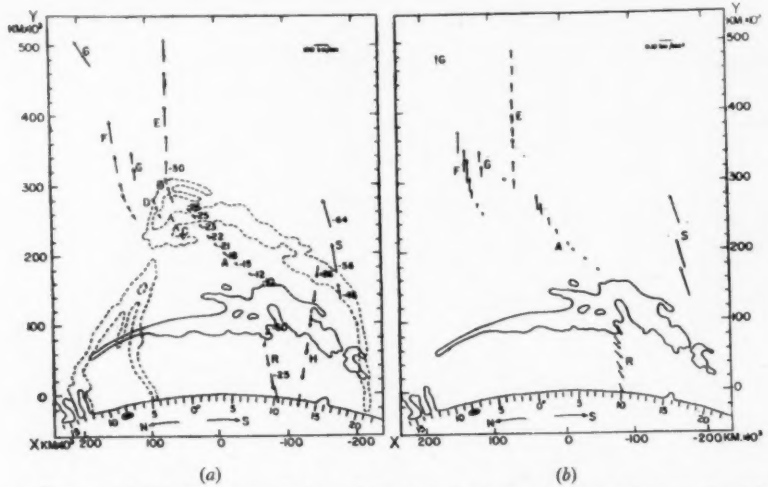

FIG. 3.—(*a*) *Velocities: magnitudes and direction of velocities in the xy-plane are shown by arrows; velocities in the z or radial direction are indicated by numerals.* (*b*) *Accelerations: magnitude and direction of accelerations in the xy-plane are shown by arrows.*

(2) *Ascending spike.*—Another secondary ejection (Feature S) took place at $17^h 10^m$. Material was apparently shot some 100,000 km. upward from a relatively immobile portion of the bright mass. Its space velocity was very great and increased from 125 to 214 km./sec. The acceleration was very large, almost 0·2 km./sec.^{2}, and was directed outward. Its form was that of an ascending bright spike and in this respect it could be said to resemble the surge-type prominence. However, the properties of this spike and those of the surge-type prominence are so different that they cannot be identified with the same activating mechanism:—

(*a*) The spike had its base in an elevated prominence, not in the chromosphere or photosphere.

(*b*) There was no evidence of the return of the material along the path of ejection, with consequent diminution in apparent height.

(*c*) The ascending motion showed an acceleration upward rather than downward, as is the case for the surge-type prominence.

5. *Evidence for Moving Material*

Intercomparisons of the geometry of the prominence, the velocities in the x, y and z directions and their changes with time provide the following data which are consistent with the hypothesis of moving material : (1) Between $15^h 45^m$ and $17^h 30^m$ the velocities in the x, y and z directions were of the same order of magnitude and all increased with time. (2) As the bright mass moved upward over the southern branch of the arch, its radial velocity was ***negative.*** After it had risen and material had begun to descend to the south along apparently the same trajectory, the radial velocity was *positive*. This change in the sign of the radial velocity can be seen clearly by comparison of the spectra for $16^h 02^m$ and $17^h 28^m$ in Fig. 1 (Plate 3). In the former the bright mass was ascending the southern branch of the prominence and at a height of 136,000 km. (well within the body of the feature, not its upper tip) the radial velocity was of the order of -30 km./sec. In the later scene, at a corresponding position on the trajectory, the radial velocity was of the order of $+70$ km./sec. These later spectra also show material descending on the northern branch of the prominence with a negative radial velocity of about 50 km./sec. These changes in the sign of the radial velocities are exactly those that would be expected if actual material were moving in the manner here described along an arching prominence whose southern tip was behind the limb of the Sun and whose northern extremity was already projected on the solar disk.

Acknowledgments

The writers acknowledge with pleasure their indebtedness to the members of the staff of the McMath-Hulbert Observatory for their constant assistance and cooperation. The continuous record of a solar phenomenon represents the culmination of many aspects of both instrumentation and observation. Sincere thanks are tendered to the McGregor Fund of Detroit for continuing grants-in-aid in support of the work of the McMath-Hulbert Observatory.

The McMath-Hulbert Observatory,
University of Michigan,
Pontiac, Michigan, U.S.A. :
1949 *December* 23.

MONOCHROMATIC MAGNITUDES OBSERVED WITH A COARSE GRATING

R. v.d. R. Woolley and K. Gottlieb

(Received 1950 January 16)

Summary

Very low dispersion spectra obtained with a coarse grating in front of a 30-inch reflector were used to determine magnitudes at 5980 A. and 4480 A. From internal evidence, and from comparisons (rather few in number) with Hogg and Mason's photoelectric work, the standard error of the mean magnitudes derived is about $\pm 0^{m}.05$. Comparison with Dr Gascoigne's work indicates that the standard error of the gradients is ± 0.08. The method is capable of extension to the tenth magnitude without unduly long exposure time.

---

1. The Reynolds 30-inch reflector of the Commonwealth Observatory at Mount Stromlo is equipped with a coarse grating. As the grating has 10 wires in 3 cm., and as the focal length of the Newtonian arrangement of the telescope is 120 inches, the grating produces little spectra at this focus with a dispersion of 9800 A./mm. This dispersion is of course very tiny, but the little spectra have certain advantages over objective prism spectra made with a refracting telescope, since the scale is not cramped in the red relative to the blue and there is no "secondary spectrum" due to chromatic aberration in the telescope. Also, the wave-length of any part of the spectrum is fixed by its distance from the central image. The resolving power in the spectra is limited by plate grain and by the performance of the telescope, and depends on the state of the figure of the mirror, the seeing and the guiding. Under good conditions, the resolution is such that the image of a truly monochromatic source would fall off to half the central intensity at about 250 A. distant on either side of the centre. Notwithstanding the tiny scale and feeble resolution it was decided to measure some grating spectra with slits sampling about 250 A. of the photographic images, in order to see whether magnitudes or gradients could be determined with a reasonably small error; because if the method were at all successful it would give a means of measuring the quantities concerned in stars down to the ninth or tenth magnitude without unduly prolonged exposures.

It was found at the outset that the consistency of the results was improved by trailing the spectra in the direction perpendicular to dispersion. The grating was therefore set to disperse perpendicular to the direction of daily motion and the telescope was trailed by driving it at three-quarters of the diurnal rate. Since the speed at which the image moved on the plate depended on the declination of the star it was necessary to perform experiments with comparison spectra trailing at different speeds to determine the reciprocity failure of the photographic plates. The spectra of various stars were brought to comparable densities by spinning appropriate sectors just inside the focus, a set of sectors cutting down by 5 magnitudes, $4\frac{1}{2}$ magnitudes and so on in $\frac{1}{2}$ magnitude steps down to $\frac{1}{2}$ magnitude being used. At least two sectors (counting no sector at all as the "0 sector")

were spun in front of each star on each plate. Each photographic plate used was calibrated in an auxiliary spectrograph, but the method depends for its accuracy on the sectors used in the stellar exposures.

The spectra appear back to back symmetrically disposed about a central trail. They were measured in a projection photometer carrying a double slit in front of the photocell, the distance between the slits being twice the wave-length required on the projected scale of the spectra. The use of a double slit makes setting easier and more reliable than is the case with a single slit. All the plates were measured with slit pairs set at 5980 A. and 4480 A., and about a quarter of the plates were also measured with a pair of slits set at 5780 A. Since the measures with the intermediate slit pair interpolated well between the two extremes, it was decided not to measure all the plates in the extra wave-length. The widths of all the slits used were about 250 A. on the projected scale of the spectra.

No attempt was made to determine atmospheric absorption. Instead, stars were observed with $1{\cdot}4 > \sec z > 1{\cdot}2$ as far as possible, and corrections of $0^{m}{\cdot}3 \sec z$ in the blue and $0^{m}{\cdot}1 \sec z$ in the red applied.

The results were tested by comparing the magnitudes of eight stars with photoelectric observations (unpublished) by Mr Hogg and Miss Mason at 4550 A. The blue coarse grating magnitudes uncorrected for the nominal wave-length difference of 70 A. show a standard error of $\pm 0^{m}{\cdot}06$ tested against these; when a correction for the wave-length difference is applied, the standard error falls to $\pm 0^{m}{\cdot}046$. Since the spectral types range from B0 to K2, the nominal wave-length of the grating magnitudes cannot be far in error. In addition to this test, the observed gradients of eight stars were compared with (unpublished) determinations by Dr Gascoigne, the standard deviation in the gradient ϕ being $\pm 0{\cdot}08$. (Six stars were common to the two lists.)

The exposure time depended only on the length of trail required, i.e. with a fixed trailing speed of the polar axis, on the declination of the star. Stars of $-60°$ declination were trailed for 20 seconds. Since the method at present reaches to the sixth magnitude, a modification which repeats the trails will go well down to the ninth magnitude with 10-minute exposures.*

The least satisfactory features of the method are reciprocity failure and waste of light. The dependence of trailing speed upon declination necessitates a separate experiment to determine reciprocity failure, and it is proposed to eliminate this feature by driving the plateholder backwards and forwards relative to the telescope, which will be driven at normal speed. This modification will admit longer effective exposure times, and extend the range of magnitudes downwards from the sixth. (The apparatus will be a one-dimensional " Schraffierkasette ", and only one dimension is available if the other is used for dispersion.)

Light is wasted by the grating; only half the starlight ever gets past the wires, and of this two-thirds goes into the central image, so that less than a tenth gets into each of the two spectra. It is intended to remove the grating and substitute a narrow-angle reflecting prism at the Newtonian flat (placed between a pair of singlet lenses of opposite power to make the light parallel and focus it again). This modification will either give more dispersion or cut down exposures on faint stars; but it will sacrifice the linear dispersion.

* *Note added* 1950 *April* 14.—The star H.D. 25224, magnitudes 9·27 red, 10·14 blue, has been measured using 15-minute exposures.

2. Each sector used in cutting down starlight is mounted permanently on the spindle of a small 6-volt D.C. motor which is carried on a substantial aluminium slide which may be pushed into a keyway in front of the plateholder. Electric contact is established only when the slider is in the correct position. Two types of plateholder were used in the series, taking quarter plates and quarter plates cut in half parallel to the longer side respectively. In the later plates in the series quarter plates cut in half were used; on these twelve stellar spectra were exposed, at least one of which was a repeat of an earlier exposure. In addition four comparison spectra were exposed. Such a plate takes about an hour to secure, more than half of the time being spent on setting the telescope.

The plates were Panatomic X developed for 4 minutes at 65 deg. F. in Kodak D26 developer.

The calibrating spectrograph is illustrated in Fig. 1. Four pinholes were mounted in a slide A at the focus of a collimator. This slide was moved horizontally by a worm and nut driven by a 50-cycle synchronous motor and suitable reduction gear. Parallel light from the collimator lens C passed onto a photograph D of the coarse grating. After passing through the photographic grating the light fell onto a small camera lens E having the same focal ratio as the Reynolds telescope, so that the spectra F of the pinholes were similar to those of the actual stars.

In front of the pinholes A a step sector B is spun by a 6-volt motor similar to those used for the star sectors. This step sector runs in half magnitude steps from $\frac{1}{2}^m$ to $3\frac{1}{2}^m$ and is mounted in a slide so that any four steps desired can be placed in front of the pinholes. The whole is illuminated by an automobile tail-light behind a blue filter and diffusing screen. In order to eliminate linear errors in the illumination, comparison spectra were secured in pairs such as:—

Hole	a	b	c	d	a	b	c	d
Step	$\frac{1}{2}$	1	$1\frac{1}{2}$	2	2	$1\frac{1}{2}$	1	$\frac{1}{2}$

It was found best to adjust the distance of the lamp from the diffusing screen so that a hole with no sector in front of it gave a slightly overexposed trail, and then to make two pairs of trails with 0^m, $\frac{1}{2}^m$, 1^m, $1\frac{1}{2}^m$ and 1^m, $1\frac{1}{2}^m$, 2^m, $2\frac{1}{2}^m$ sectors in front of the holes. There are then six points on the calibration curve for the plate and the usable range of densities is well covered.

The heights of the steps were equal to the distances between consecutive holes, and greater than the distance trailed by a comfortable margin.

Intermittency.—Nearly all the spectra were secured with intermittent exposures, the only exceptions being the 0^m spectra in comparison images and some faint stars on which the sectors used were 0^m and $\frac{1}{2}^m$ (or 0^m and 1^m). No systematic difference was found.*

Reciprocity failure.—Four worms and nuts, with pitches of $\frac{1}{40}$ inch, $\frac{1}{20}$ inch, $\frac{1}{10}$ in. and $\frac{1}{6}$ inch were employed to drive the pinhole slide A. These trailed the comparison spectra F at the same speed on the plate in mm./sec. as the telescope trailed stars of declination 82° 31′, 74° 48′, 58° 22′ and 29° 01′. Considering any particular point on the trail, the time integral of the amount of light received

* The running of the motor depends on the state of the bearings and also on the position (relative to gravity) in which it is held. When running well the motor attains 3500 r.p.m., and when the rate falls so low as 2500 r.p.m., the motor labours audibly. When this occurred the motor was withdrawn from service next day and repaired or replaced. All sectors except one (5 mag.) carried two cuts so that the intermittency was, in these cases, doubled.

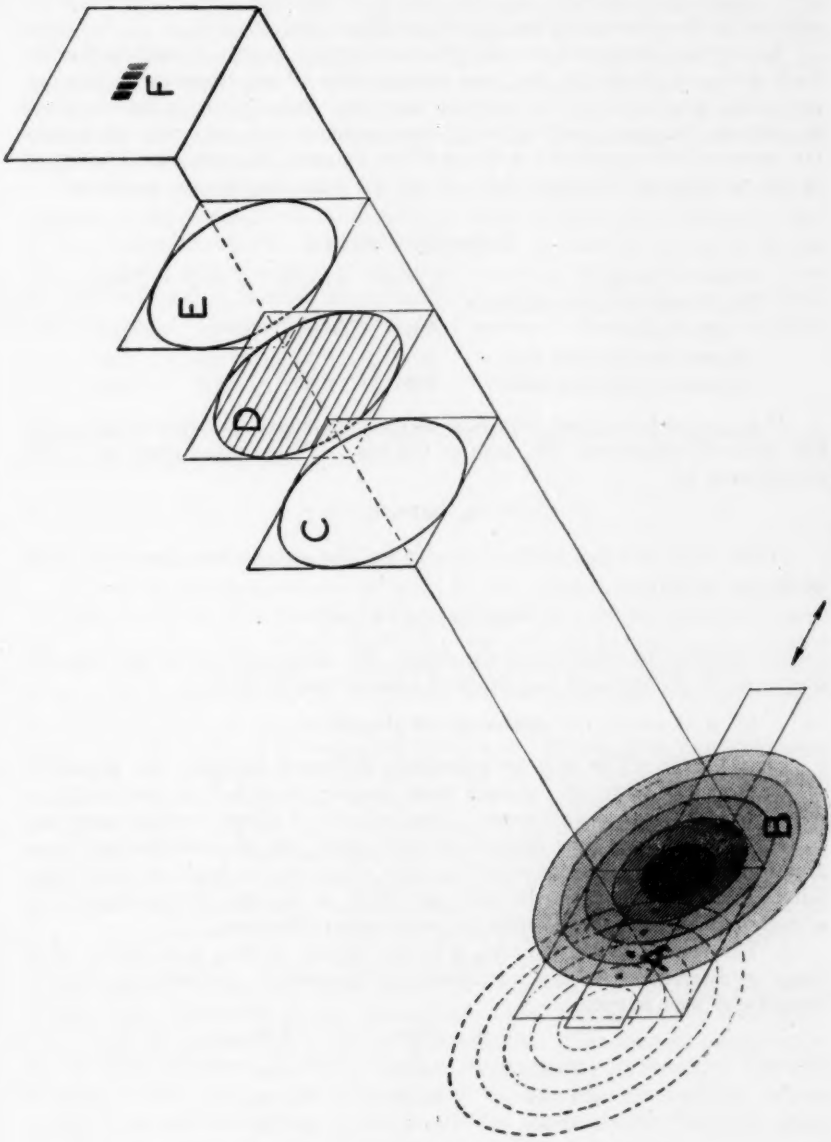

FIG. 1.—*The calibrating apparatus.*

is inversely proportional to the speed of the image, and the brightness of the images integrated in this way are

$$0^{m}\cdot00, \quad +0^{m}\cdot76, \quad +1^{m}\cdot51, \quad +2^{m}\cdot06,$$

referred to the slowest moving ($\frac{1}{40}$ inch pitch) as zero.

Seven plates were taken, on each of which were 64 spectra, 16 with each pitch. Each group of 16 spectra had four arrangements of the sectors and pinholes, and could be used in itself to calibrate the plate. Selecting any particular pitch to calibrate the plate, each set of 16 spectra taken with any other pitch gives (16 values of) the apparent brightness of the sources. All plates were measured in the red (6000 A.) and blue (4500 A.) and the mean results were as follows :

Reciprocity Failure

Pitch of Screw	$\frac{1}{40}$ inch	$\frac{1}{20}$ inch	$\frac{1}{10}$ inch	$\frac{1}{6}$ inch
Brightness with zero reciprocity failure	$0^{m}\cdot00$	$0^{m}\cdot76$	$1^{m}\cdot51$	$2^{m}\cdot06$
Apparent brightness, red	0·00	0·54	1·12	1·57
Apparent brightness, blue	0·00	0·54	1·11	1·59

If m_c is the brightness with zero reciprocity failure in magnitudes and m_0 the apparent brightness, the mean of the red and blue taken together is well represented by

$$m_0 = 0{\cdot}75\, m_c.$$

If the plates are taken individually and the best straight line adopted for each plate, the result is

$$m_0 = (0{\cdot}77 \pm 0{\cdot}03) m_c,$$

which indicates the reliability of the result. We adopt $m_0 = 0{\cdot}76\, m_c$ and then the correction to the apparent magnitude of a star of declination δ is

$$\Delta m = 0{\cdot}76 \times 2{\cdot}5 \log \sec \delta.$$

Closing error.—The average magnitude difference between two exposures of the same star taken on the same plate (usually about half an hour apart) is $0^{m}\cdot07$, from 75 such comparisons. This includes of course possible variations in the sky during the time taken to secure a plate, but the contributions from atmospheric reddening as distinct from thin cloud are not large, as the average failure to close is $0^{m}\cdot08_5$ in the blue and $0^{m}\cdot06_6$ in the red. If the errors were entirely atmospheric there would be more colour difference.

3. The stars α Tr Au, β Tr Au, γ Tr Au, β Pavo, γ Pavo and δ Pavo were taken as reference stars and intercompared frequently; the following relative magnitudes were adopted:—

	Blue	Red
	m	m
α Tr Au	0·00	0·00
β Tr Au	−0·05	+1·14
γ Tr Au	−0·23	+1·26
β Pavo	+0·39	+1·74
γ Pavo	+1·51	+2·47
δ Pavo	+1·01	+1·68

and all the remaining magnitudes have been determined with reference to one of these stars. The results for 34 stars obtained from 44 plates exposed between 1949 July 7 and 1949 September 17 are shown in Table I. The qualification for a star appearing in this table is its measurement on at least three plates. The zeros of the magnitude scales have been adjusted so as to make the average difference between the magnitudes of the four A0 stars observed and the magnitudes of these stars in the Harvard Mimeograph catalogue zero in both colours. No standard error is shown for α Tr Au, and the standard errors shown for the remaining five reference stars are the standard errors of their magnitudes relative to α Tr Au.

The table shows the results of 182 determinations. The sums of all the squares of the residuals of the individual determinations of a particular star from the adopted value for the star are 20,988 in the blue and 26,042 in the red (the unit being a hundredth of a magnitude squared), so that the average value of $\Sigma v^2/n$ is found by dividing those numbers by 182. The results are 115 (blue) and 143 (red). The standard errors of the means of observations are therefore

$$\sqrt{115/(n-1)} \quad \text{and} \quad \sqrt{143/(n-1)}$$

respectively, the unit being a hundredth of a magnitude. For example, with $n=6$, the average standard errors are

$$\pm 0^{m}{\cdot}048 \quad \text{and} \quad \pm 0^{m}{\cdot}053$$

in the blue and red respectively.

Monochromatic magnitudes for stars in the Hyades and in the region of Praesepe have been determined by Ramberg (*Stockholms Observatoriums Annaler*, **13,** No. 9, 1941). He used an objective prism attached to the 40-cm. refractor at Stockholm. On account of chromatic aberration in the object glass, only a portion of the spectrum was in good focus, and the magnitudes were determined at 4215 A. for spectral classes B to F and at 4360 A. for classes G to M. The equipment reached stars of magnitude $13^{m}{\cdot}5$ in the Hyades, with standard errors of $0^{m}{\cdot}050$ for the early-type stars and $0^{m}{\cdot}058$ for later types; in the Praesepe region the limiting magnitude was $13^{m}{\cdot}0$, and the standard errors $0^{m}{\cdot}038$ and $0^{m}{\cdot}045$ for early and late stars respectively. The dispersion used was about 200 A./mm. and the exposure time for the faintest star was two hours. In comparing Ramberg's standard errors with those in the present work, one must recognize that comparisons between stars well separated in the sky may be expected to exhibit considerably larger errors than comparisons in a restricted region photographed together, other things being equal.

4. Eight of the stars in Table I have been observed by Mr Hogg and Miss Mason with a photoelectric cell placed behind an aperture in the focal plane of the slitless spectrograph on the 30-inch reflector. This aperture passes 100 A. of the stellar spectrum, centred on 4550 A. Comparisons are shown in Table II between relative magnitudes observed with the photocell (preliminary values, subject to revision) and those observed with the coarse grating, the latter being shown both uncorrected for the wave-length difference between 4550 A. and 4480 A. and corrected for this difference by subtracting $0{\cdot}038\phi$, the gradient ϕ being taken from Table I.

TABLE I

Observed Magnitudes

Star	Spectrum	Mag. (5980 A.)	Mag. (4480 A.)	Standard errors (in 100ths of a Mag.) Red	Blue	No. of plates	*HM*	ϕ
π Tucn	B9	5·66	5·65	6·4	7·0	3	5·32	−0·02
λ Hydi	K5	4·77	6·35	2·0	5·3	3	4·76	+2·27
α Erid	Bo	0·73	0·52	5·8	5·2	7	0·60	−0·35
η Circ	G5	5·05	5·98	3·5	1·3	5	5·11	+1·53
ϵ Circ	Ko	4·73	5·96	6·1	11·8	3	4·68	+2·01
γ Tr Au	Ao	3·07	3·08	6·5	3·2	8	2·98	+0·02
ϵ Tr Au	Ko	3·96	5·22	4·5	6·3	5	3·95	+2·08
β Tr Au	Fo	3·00	3·27	7·1	2·7	9	2·97	+0·44
δ Tr Au	Go	3·70	4·89	3·7	9·7	5	3·93	+1·96
ζ Tr Au	Go	4·94	5·54	8·9	12·0	3	4·83	+0·99
γ Apus	Ko	3·79	4·74	8·9	7·8	3	3·74	+1·56
β Apus	Ko	4·06	5·40	3·4	6·9	5	4·00	+2·24
α Tr Au	K2	1·81	3·31	...	...	8	1·72	+2·47
ι Apus	B_8	5·60	5·60	10·7	3·0	3	5·49	0·00
δ Arae	B_8	3·87	3·76	9·3	11·7	5	3·68	−0·18
η Pavo	Ko	3·57	4·83	5·3	5·3	9	3·42	+2·08
ϕ Octn	Ao	5·58	5·61	4·4	3·4	7	5·53	+0·05
ϵ Sgtr	Ao	1·90	1·94	5·0	5·2	3	1·95	+0·07
ζ Pavo	Ko	3·94	5·20	6·3	5·0	8	3·94	+2·08
θ Pavo	A3	5·75	6·09	9·4	6·4	5	5·84	+0·56
λ Pavo	B2	4·27	4·18	3·5	3·6	7	4·28	−0·15
ϵ Pavo	Ao	3·92	3·86	7·4	4·0	5	4·02	−0·10
δ Pavo	G5	3·49	4·32	4·1	3·8	9	3·53	+1·37
β Pavo	A5	3·55	3·70	3·0	2·1	9	3·56	+0·25
α Octn	F2	5·23	5·71	2·2	2·6	6	5·17	+0·79
o Pavo	Ma	4·68	6·50	6·2	3·7	5	4·84	+3·00
γ Pavo	F_8	4·28	4·82	2·8	2·3	10	4·22	+0·89
ν Octn	Ko	3·53	4·63	5·9	3·0	3	3·59	+1·81
ψ Octn	A5	5·56	5·77	2·1	2·3	3	5·58	+0·35
α Tucn	K2	2·74	4·28	2·3	4·8	6	2·74	+2·54
ν Indi	Go	5·18	5·99	6·3	3·2	6	5·33	+1·33
β Octn	Fo	4·29	4·48	3·2	2·0	5	4·28	+0·31
γ^1 Octn	G5	5·01	6·04	4·0	2·1	3	4·99	+1·69
γ^2 Octn	Ko	5·64	6·73	5·2	0·9	3	5·52	+1·79

TABLE II

Comparison of Coarse Grating Magnitudes with Photocell

Star	Spectrum	Photoelectric 4550 A.	Coarse grating 4480 A.	Photocell minus grating	Coarse grating corrected to 4550 A.	Photocell minus corrected grating
		m	m	m	m	m
α Erid	Bo	−1·47	−1·52	+0·07	−1·51	+0·06
δ Arae	B_8	+1·71	+1·72	−0·01	+1·73	−0·02
ϵ Sgtr	Ao	0·00	−0·10	+0·10	−0·10	+0·10
γ Tr Au	Ao	+1·05	+1·04	+0·03	+1·04	+0·01
β Pavo	A5	+1·71	+1·76	−0·05	+1·75	−0·04
β Octn	Fo	+2·44	+2·44	0·00	+2·43	+0·01
δ Pavo	G5	+2·23	+2·28	−0·05	+2·23	0·00
α Tr Au	K2	+1·15	+1·27	−0·10	+1·17	−0·02

The root mean square of the "uncorrected" residuals is $\pm 0{\cdot}06_2$, and that of the "corrected" residuals is $\pm 0{\cdot}04_6$. The agreement is very satisfactory

and shows that there is no difference in scale over 4 magnitudes and also (since a wide range of spectral type is concerned) that the blue grating magnitudes are very close to being monochromatic magnitudes, despite the low resolution.

Eight of the stars have been measured in Dr Gascoigne's relative gradient programme, also carried out on the 30-inch reflector. The relative gradient between two stars is defined by

$$\phi = \frac{1}{1{\cdot}086}\,\frac{\Delta m_r - \Delta m_b}{(1/\lambda_r - 1/\lambda_b)}.$$

TABLE III

Comparison of Gradients

Star	Spectrum	ϕ, Gascoigne	ϕ, Coarse grating	Diff. Gascoigne minus Coarse grating	Diff. minus 0·08
α Erid	Bo	−0·24	−0·35	+0·11	+0·03
λ Pavo	B2	−0·10	−0·15	+0·05	−0·03
δ Arae	B_8	−0·14	−0·18	+0·04	−0·04
ϵ Sgtr	Ao	+0·04	+0·07	−0·03	−0·11
γ Tr Au	Ao	+0·03	+0·02	+0·01	−0·07
β Tr Au	Fo	+0·68	+0·44	+0·24	+0·16
β Pavo	A5	+0·37	+0·25	+0·12	+0·04
δ Pavo	G5	+1·43	+1·37	+0·06	−0·02

The mean difference is (Gascoigne minus Coarse Grating) +0·08 indicating a difference in the adopted zeros of the scales. The differences between the relative gradients are shown in the last column, the root mean square being $\pm 0{\cdot}07_7$. As the standard error of the Greenwich gradient determinations is $\pm 0{\cdot}03$, this comparison is quite satisfactory.

5. Fig. 2 shows gradients plotted against spectral type, and Fig. 3 shows the difference between the magnitudes interpolated to 5500 A. and the Harvard Mimeograph magnitudes plotted against gradients. There is a very marked dependence of the difference Stromlo minus HM on spectral type. This

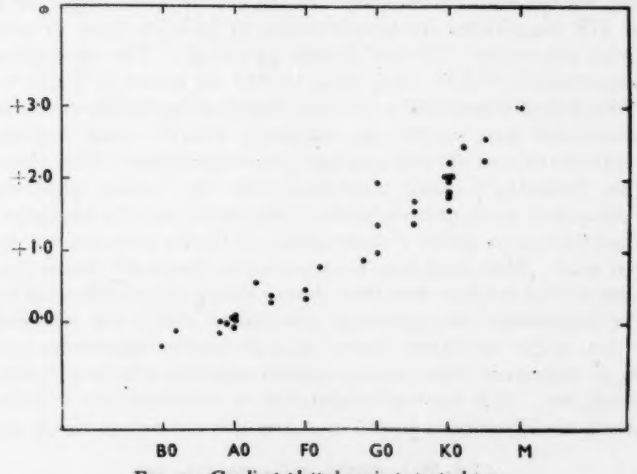

FIG. 2.—*Gradient plotted against spectral type.*

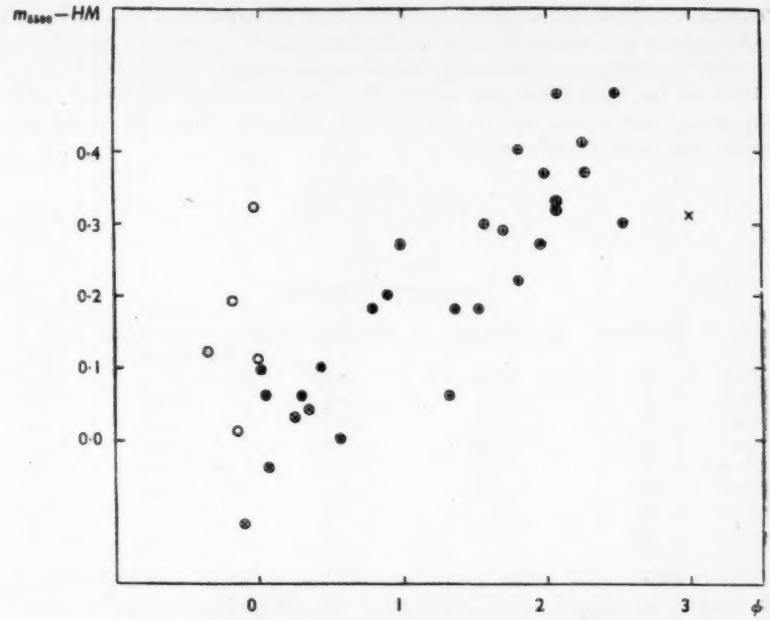

FIG. 3.—*Comparison with Harvard Mimeograph magnitudes. The magnitudes interpolated to* 5500 A. *are shown plotted against the gradient* ϕ, *various symbols representing the spectral type.*

M K G F A B

× ● ● ● ● ○

difference is actually decreased if the earlier Harvard magnitudes HR are substituted for the more recent ones. In the case of these bright, far southern stars, the HR magnitudes are simple means of Bailey's visual determinations with a 4-inch photometer (*Harvard Annals*, **34** and **46**). The corrections applied to the magnitudes in HR to bring them to HM are shown in Table V of Miss Payne's *Photovisual Magnitudes in Harvard Standard Region* (*Harvard Annals*, **89**). These corrections were derived by comparing Bailey's visual magnitudes for 98 stars between 6^m and 9^m with standard photovisual stars. Miss Payne's table shows that Pickering's colour correction with the 12-inch photometer was strongly dependent on magnitude between 7^m and 9^m, and it is suggested that the adopted corrections to Bailey's observations of fainter stars are not applicable to brighter stars. This conclusion is supported by Cousins *, whose photovisual magnitudes of stars brighter than $6^m{\cdot}0$ show a strong colour difference with HM.

6. The magnitudes and gradients, determined with a low resolving power such as this, might be called coarse monochromatic magnitudes and coarse gradients, to distinguish them from quantities observed with instruments having higher resolution. It is however undesirable to introduce new technical terms when there is small justification, and moreover it is not certain where one should

* A. W. J. Cousins, *M.N.*, **103**, 154, 1943.

draw the line between a coarse monochromatic magnitude (or oligochromatic magnitude) and a " monochromatic " magnitude. If the spectra were free from absorption lines, the simple and obvious definition of a monochromatic magnitude would be useful: but since stars do show absorption lines, for many purposes one does not wish to ascertain the light flux in a narrow range of frequencies which might fall within a line. The average value of this quantity over a range of frequencies large enough to sample the incidence of lines fairly may therefore be of far more value. We do not wish to labour this difficulty, but think it of sufficient weight to be considered when contemplating the introduction of qualifying adjectives to the term " monochromatic magnitudes ". Regarding the coarse gradients, we feel that they are much closer to (accurate) gradients than they are to colour indices, because the spectral ranges considered are much more definite than those employed by instruments which take in a wide enough spectral range to be appreciably influenced by variations with wave-length of transmission in the Earth's atmosphere and in glass, or in the reflectivity of silver.

While, then, the authors expect the magnitudes and gradients determined with the low resolution they have used to show (small) differences from determinations made with higher resolving power, they have not thought it advisable to introduce special qualifying nomenclature.

Acknowledgments.—The authors are particularly indebted to Mr J. H. Banham for the care with which he has supervised the construction of the apparatus, and to Miss Janet Lamb for measuring many of the plates. They also acknowledge with pleasure their indebtedness to Mr Hogg, Dr Gascoigne, Mr Stibbs and Miss Mason who have helped in a number of ways.

Commonwealth Observatory,
Mount Stromlo, Canberra :
1950 *January* 10.

ON THE INTERPRETATION OF MEASURED SOLAR WAVE-LENGTHS

Lyman Spitzer, Jr.

(Received 1950 January 13)

Summary

Reasons are given for expecting that collisions with *H* and *He* atoms produce a shift of most Fraunhofer lines to the violet rather than to the red. When allowance is made for this effect, and for the many uncertainties in collisional broadening theory, the interferometric measures of solar wave-lengths seem consistent with a complete absence of systematic Doppler shifts on the solar surface.

In a recent thorough-going and important study, Miss Adam (**1**) has measured with an interferometer the precise wave-lengths of 14 lines in the solar spectrum at 14 distances from the centre of the disk. For $\cos\theta$ equal to 0·181, comparison between solar and laboratory wave-lengths shows an average red shift of 0·0129 A., the exact value predicted by general relativity theory. With increasing distance from the limb the red shift was found to diminish, and at the centre of the disk amounted to less than half of the relativity shift.

In the theoretical interpretation which Miss Adam develops for these observations, a substantial correction is made for the shifts produced by collisions between absorbing atoms and atomic *H*. The line shift, assumed to be toward the red in all cases, is set equal to $0{\cdot}36\gamma$, where γ is the collisional damping constant and the factor 0·36 is from a theory by Lindholm (**2**). Values of γ at different distances from the limb are taken from the observational study of strong *Fe* lines by ten Bruggencate and Houtgast (**3**). Since γ is greatest at the centre of the disk, where we see down into deeper layers in which collisions are more frequent, the theoretical collisional red shift is greatest near the centre of the Sun. Since the observations show a red shift which is actually least at the centre, appreciable upwards velocities, at least 0·5 km./sec., seem indicated. However, such velocities are too great to be reconciled with existing theories of the solar atmosphere.

The theory of collisional perturbations on absorption lines plays a major part in this analysis. The following brief summary of relevant information on this subject indicates that certain modifications seem appropriate in the theory used by Miss Adam.

The shift of absorption lines in the presence of atoms of a foreign gas has been known for some time. Observations and theories in this field have been summarized by Weisskopf (**4**) and by Margenau and Watson (**5**). This latter survey also presents the previous theory of Margenau, which accounts for the observed fact that the shift of a broadened line averages a little less than one-half of the half-width. The subsequent contribution by Lindholm (**2**) lies not in discovering this proportion between shift and half-width, but rather in presenting a simplified form of collisional broadening theory, in which the ratio of collisional

shift to collisional half-width may be computed for any assumed law of interaction between the colliding atoms. This same theory has also been presented independently by Foley (**6**). When the perturbing force varies as the inverse sixth power of the separation, as may be expected for interaction at great distances between *H* and other atoms, this theoretical ratio becomes 0·36.

It should be emphasized that this theoretical result is only an approximation. In the first place the theory, while a considerable improvement over previous theories, is still drastically over-simplified. A discussion of the theoretical problems involved is given in Unsöld's survey article (**7**) on collisional effects in spectral lines. Moreover, the observations, which have been summarized by Foley (**6**), show a very large scattering of this ratio about the theoretical value, with values ranging from 0·16 to 0·77. While the average ratio is 0·38, in close agreement with the Lindholm-Foley theory, any use of a constant ratio involves the possibility of very considerable error.

The direction of shift, obviously a matter of great importance, will depend on the difference in perturbation between the upper and the lower levels of the transition producing the line in question. If the force between the two atoms is attractive, the energy levels will be depressed. The usual van der Waals forces will depress the upper level more than the lower one, and the line will be shifted to the red. This corresponds with the observed fact that almost all resonance lines are shifted to the red by the presence of a foreign gas.

For levels of high excitation the van der Waals theory is not applicable, since the radius of the electron orbit becomes so large that a perturbing *H* atom passes inside this orbit during a typical collision. The theory for a highly excited level (*n* equal to 15 or more) has been considered by Fermi (**8**) and Reinsberg (**9**). The computations show that the sign of the dominant term in the perturbation energy depends on the phase shift δ of the wave function for a free electron when such an electron is scattered by the perturbing atom. If $\tan\delta$ is negative, the energy level is raised, with a violet shift resulting. Observations show that the higher members of the principal series in the alkali metals are shifted to the violet by *He* and *Ne*, and to the red by *A*, *Kr* and *Xe*. The discussion by Reinsberg (**9**) indicates that these results are in good quantitative agreement with the theory.

While there are no available observations on collisional shifts of this type produced by *H*, the theory may be applied in this case also. Wave functions for a free electron in the field of an *H* atom have been computed by Morse and Allis (**10**); electron exchange was taken into account, but separable wave functions were used. A simplified form of non-separable wave function, which neglects electron exchange, has been considered by Huang (**11**). Both of these results show a phase shift decreasing monotonically from 180° at zero energy to a low value at high kinetic energies, a result similar to that found for *He*. Thus $\tan\delta$ is negative for electrons of low energy. It follows that collisions with *H* atoms will produce shifts to the violet in any absorption line to a highly excited state, near the ionization limit. This result does not seem to have been realized previously.

For lines arising from transitions between levels of intermediate excitation there is at present no adequate theory available. Observations on the spectra of alkali metals indicate that where violet shifts appear at all they appear in all lines except the resonance line. Specifically, when *He* is the perturbing gas, the second and all higher members of the 6s–np series of *Cs* (**12**) and the second member

of the 5s–np series of *Rb* (**13**) are shifted to the violet; for *K* (**14**) the measures extend down only to the third line of the 4s–np series, but the violet shift of this line exceeds the shift near the series limit. Thus violet shifts of most absorption lines seem probable when an atom is perturbed by *H* or *He*.

While collisional violet shifts seem likely in the Sun, no precise theoretical prediction of such shifts is presently possible. One may nevertheless ask whether Miss Adam's measured shifts are consistent with the belief that no systematic Doppler shifts are present, and that the observed values of Δ, the red shift measured in units of 0·001 A., are the combined effect of collisional shifts and the Einstein gravitational shift.

To answer this question we first repeat Miss Adam's analysis of her data, changing the sign of the collisional shift but retaining all her other assumptions. The apparent Doppler shifts resulting are given in Table I below, which follows closely the form of Miss Adam's Table V. It is evident that the resultant velocities are now only about one-third of those previously found.

TABLE I

Mean Line Shifts and Radial Velocities

$\cos\theta$	Mean obs. Δ	Collisional shift	Residual Δ	Velocity shift and p.e.	Velocity v_θ km./sec.
1·000	5·0	−4·1	9·1	−3·8±0·5	−0·186±0·026
0·817	5·3	−3·8	9·1	−3·8±0·6	−0·186±0·029
0·639	5·2	−3·4	8·6	−4·3±0·6	−0·211±0·029
0·468	5·9	−2·9	8·8	−4·1±0·6	−0·201±0·031
0·398	7·2	−2·6	9·8	−3·1±0·6	−0·152±0·032
0·282	9·1	−2·1	11·2	−1·7±0·7	−0·083±0·032
0·181	12·9	−1·5	14·4	+1·5±0·7	+0·074±0·032

Three additional modifications must also be considered. Firstly, there may be a systematic error either in the solar wave-lengths or in the laboratory values. Since the observed value of Δ at $\cos\theta = 0{\cdot}181$ is just equal to the value predicted from general relativity, it is evident that this value of Δ must be in error if collisional shift is assumed present without any Doppler shift. Secondly, the damping constant for the lines investigated need not be the same as for the lines studied by ten Bruggencate and Houtgast (**3**), since considerable scatter of damping constant may be expected from one line to another because of variation with atomic properties. Thirdly, the ratio between collisional shift and damping constant may differ markedly from the theoretical value. With so many uncertainties in the theoretical interpretation, the resultant Doppler velocities can evidently be reduced to a low value.

On the basis of the evidence available one may conclude that Miss Adam's observations are consistent with the belief that motions in the solar atmosphere (excluding rotation and small-scale phenomena near sunspots) are so slight that the measured shifts are simply the sum of the relativity red shift and a collisional violet shift. On the other hand, these shifts are not inconsistent with moderate Doppler shifts of some 0·2 km./sec. As suggested by Richardson and Schwarzschild (**15**), effective shifts of this order could be produced by rapid convective currents with a scale much smaller than the observable granules. The assumption that both Doppler shifts and collisional shifts are present is consistent with the extensive observational material obtained by Adams (**16**)

on the red shift of Fraunhofer lines at the Sun's limb relative to the centre. The relatively low shifts found for lines formed high in the Sun's atmosphere, where large turbulent velocities might be expected, would seem somewhat unfavourable to the hypothesis that Doppler shifts alone could account for the centre-limb variations.

Princeton University Observatory:
1949 *December* 23.

References

(1) M. G. Adam, *M.N.*, **108**, 446, 1948.
(2) E. Lindholm, *Arkiv. f. Mat. Astr. och. Fys.*, **28B**, No. 3, 1941.
(3) P. ten Bruggencate and J. Houtgast, *Z. f. Ap.*, **20**, 149, 1940.
(4) V. Weisskopf, *Phys. Zeits.*, **34**, 1, 1933.
(5) H. Margenau and W. W. Watson, *Reviews of Modern Physics*, **8**, 22 and 398, 1936.
(6) H. M. Foley, *Phys. Rev.*, **69**, 616, 1946.
(7) A. Unsöld, *V.J.S.*, **78**, 213, 1943.
(8) E. Fermi, *Nuovo Cim.*, **11**, 157, 1934.
(9) C. Reinsberg, *Z. f. Phys.*, **93**, 416, 1935.
(10) P. M. Morse and W. P. Allis, *Phys. Rev.*, **44**, 269, 1933.
(11) Su-Shu Huang, *Phys. Rev.*, **76**, 477, 1949.
(12) C. Furtchbauer and F. Gossler, *Z. f. Phys.*, **87**, 89, 1933.
(13) Ny Tsi-Zé and Ch'en Shang-Yi, *Phys. Rev.*, **52**, 1158, 1937.
(14) C. Furchtbauer and W. von Heesen, *Z. f. Phys.*, **113**, 323, 1938.
(15) R. S. Richardson and M. Schwarzschild, *Ap. J.*, **111**, 351, 1950.
(16) W. S. Adams, *Ap. J.*, **31**, 30, 1910.

THE CAPE AND RADCLIFFE OBSERVATIONS OF THE ECLIPSE COMET (1948 l)

J. v. B. Lourens and T. W. Russo

(Communicated by H.M. Astronomer at the Cape of Good Hope)

(Received 1950 January 2)

Summary

Positions are given for the Eclipse Comet 1948 l derived from plates taken at the Cape Observatory with various telescopes between 1948 November 8 and 1949 March 2, and plates taken with the 74-inch reflector of the Radcliffe Observatory, Pretoria, between 1948 December 2 and 1949 April 2. All the plates were measured and reduced at the Cape Observatory.

Table I gives the observed position of Comet 1948 l on 41 occasions between 1948 November 8 and 1949 April 2. The first three columns give the universal time of the observations and the measured positions reduced to the FK3 system and referred to the equinox at the beginning of the year. The three columns headed A, B and H give the number of exposures measured, the number of reference stars used and the hour angle of the comet, while the sixth and final columns, respectively, give the weight and the estimated magnitude, assigned to the observed position, unit weight corresponding to a probable error in position of $\pm 0''\cdot 3$. The positions given still require corrections for:—

(1) aberration due to the Earth's motion,

(2) the time taken by light in passing from the comet to the Earth,

(3) parallax.

The correction for parallax can be deduced from the quantities given in the last two columns but one of the table by dividing them by the geocentric distance of the comet. The tabulated quantities were computed from the formulae

$$\Delta . p_\alpha = +0^s\cdot 4873 \sin H \sec \delta,$$
$$\Delta . p_\delta = -4''\cdot 885 \cos \delta - 7''\cdot 309 \sin \delta \cos H$$

for the Cape observations and from

$$\Delta . p_\alpha = +0^s\cdot 5287 \sin H \sec \delta,$$
$$\Delta . p_\delta = -3''\cdot 806 \cos \delta - 7''\cdot 931 \sin \delta \cos H$$

for the Radcliffe observations.

The observations at the Cape were made with three instruments: the 5-inch Wide-Angle Astrographic Camera (scale 1 mm. = $102''\cdot 52$), the 13-inch Astrographic Refractor (scale 1 mm. = $59''\cdot 81$) and the 24-inch Victoria Refractor (scale 1 mm. = $30''\cdot 62$). From November 8 to December 13 the comet was photographed with both the first two of these instruments and one plate (containing several exposures) from each instrument was measured for each night,

TABLE 1

Cape Observations: (*Long.* $-1^h\ 13^m\ 55^s$, *Lat.* $-33°\ 56'\ 03''$)

Date (U.T.)	R.A.	Dec.	A	B	Wt.	H	$\Delta . p_\alpha$	$\Delta . p_\delta$	Mag.
1948	1948·0								
	h m s	° ′ ″				h m	s	″	
Nov. 8·11054	13 25 21·1	−21 18 35·0	4	6	0·3	−6 23·6	−0·520	−4·82	1·8
9·10104	13 17 22·4	−22 6 44·0	2	3	0·2	−6 25·4	−0·523	−4·83	2·0
10·09404	13 9 23·1	−22 54 16·3	2	5	0·3	−6 23·6	−0·526	−4·79	2·1
13·09287	12 45 13·84	−25 12 43·0	6	6	1·0	−5 49·3	−0·538	−4·27	2·7
14·10464	12 37 4·44	−25 57 22·4	4	6	0·8	−5 20·2	−0·534	−3·84	2·8
15·08394	12 29 9·83	−26 39 29·8	3	7	0·7	−5 38·2	−0·543	−4·05	3·0
17·09345	12 12 52·59	−28 2 11·4	6	1	0·3	−5 0·3	−0·533	−3·43	3·4
19·07219	11 56 43·80	−29 18 10·7	5	5	1·0	−5 7·0	−0·544	−3·44	3·8
22·07665	11 31 56·90	−31 1 52·0	6	6	1·2	−4 23·9	−0·519	−2·65	4·3
24·09747	11 15 4·36	−32 2 36·1	6	6	1·2	−3 29·1	−0·455	−1·77	4·6
26·08575	10 58 19·14	−32 54 30·2	5	6	1·1	−3 21·4	−0·447	−1·57	5·0
27·06825	10 49 59·66	−33 17 2·9	5	7	1·2	−3 34·4	−0·469	−1·70	5·2
28·06398	10 41 31·80	−33 37 44·4	6	5	1·0	−3 28·1	−0·461	−1·58	5·3
Dec. 2·04484	10 7 36·56	−34 37 15·1	8	5	1·2	−3 6·1	−0·430	−1·16	6·0
8·05688	9 17 25·89	−34 53 14·2	4	4	1·0	−1 34·8	−0·239	−0·18	6·9
13·07266	8 38 27·73	−34 1 35·2	6	4	1·1	−0 13·4	−0·034	+0·03	7·6
14·04005	8 31 23·92	−33 45 40·4	3	4	1·0	−0 49·4	−0·125	−0·09	7·7
15·04456	8 24 14·33	−33 27 23·2	3	4	1·0	−0 31·8	−0·081	−0·08	7·8
21·87236	7 40 46·42	−30 44 39·5	3	4	1·0	−3 29·4	−0·449	−1·92	8·7
29·88343	7 1 33·54	−26 44 45·6	4	4	1·0	−2 2·7	−0·278	−1·53	9·7
30·93265	6 57 18·31	−26 11 54·0	4	4	1·0	−0 43·4	−0·102	−1·21	9·8
1949	1949·0								
Jan. 5·91450	6 36 33·92	−23 5 30·8	4	6	1·0	−0 25·1	−0·058	−1·64	10·4
9·90193	6 25 36·57	−21 5 20·1	3	3	0·8	−0 16·6	−0·038	−1·93	10·8
10·89003	6 23 12·52	−20 36 20·8	3	7	1·0	−0 27·4	−0·062	−2·02	10·9
23·84553	6 0 57·02	−14 52 25·9	3	4	0·8	−0 18·2	−0·040	−2·85	12·1
31·81252	5 53 45·09	−11 55 21·9	2	3	0·6	−0 27·1	−0·059	−3·28	12·8
Feb. 3·83591	5 51 58·40	−10 54 37·3	2	6	0·5	+0 20·3	+0·044	−3·42	13·0
4·82225	5 51 29·68	−10 35 34·0	2	5	0·3	+0 5·0	+0·011	−3·46	13·1
5·82338	5 51 2·96	−10 16 31·6	2	5	0·4	+0 11·0	+0·024	−3·50	13·2
7·80940	5 50 18·33	− 9 39 51·4	2	4	0·4	−0 0·5	−0·001	−3·59	13·3
15·79840	5 48 52·11	− 7 25 32·3	2	4	0·4	+0 16·5	+0·035	−3·90	13·8
16·80959	5 48 50·59	− 7 9 55·8	2	5	0·4	+0 36·7	+0·078	−3·95	13·9
17·84287	5 48 51·00	− 6 54 16·3	2	4	0·4	+1 28·7	+0·185	−4·04	14·0
Mar. 2·79542	5 51 19·91	− 4 2 3·3	2	3	0·2	+1 8·9	+0·145	−4·38	14·5

Radcliffe Observations: (*Long.* $-1^h\ 52^m\ 55^s$, *Lat.* $-25°\ 47'\ 18''$)

1948	1948·0								
Dec. 2·99954	9 59 30·1	−34 45 47·7	1	4	0·4	−3 20·3	−0·494	−0·22	6·0
1949	1949·0								
Feb. 22·79889	5 49 18·47	− 5 43 22·1	2	4	0·5	+1 23·4	+0·189	−3·05	14·2
Mar. 3·76212	5 51 40·32	− 3 50 47·5	2	3	0·4	+1 3·5	+0·145	−3·28	14·5
15·75890	5 57 12·76	− 1 47 33·6	2	5	0·5	+1 40·6	+0·225	−3·58	15·0
23·75984	6 2 1·37	− 0 40 11·5	1	3	0·3	+2 8·6	+0·281	−3·73	15·5
30·80538	6 6 49·60	+ 0 10 36·8	1	2	0·2	+3 37·2	+0·429	−3·82	16·0
Apr. 2·80052	6 9 0·27	+ 0 29 58·4	2	4	0·5	+3 39·8	+0·433	−3·85	16·0

except on November 9 when only the Astrographic Refractor plate was measured and on November 13 when two plates from each instrument were measured. For the first three observations the comet was very bright and only 7° above the

horizon. Accurate measurements of its position were therefore very difficult, especially in right ascension, as the direction of the tail was mainly east to west.

From December 14 onwards the observations were made with the Victoria Telescope. Up to December 14 the telescope was guided on the comet and the stars allowed to trail; after December 14 a star was used for guiding and the comet allowed to trail. For the last four Cape observations neutral filters were used to reduce the brightness of the comparison stars. These filters were prepared by fogging photographic plates and then removing the film from a small area in the centre through which the comet was exposed. One such filter reduced the apparent brightness of the comparison stars by 2·8 magnitudes and two filters by 5·5 magnitudes. An exposure of from 14 to 30 minutes was required to record the comet on Ilford Astronomical Zenith Plates which had been sensitized with mercury vapour.

The observations at Pretoria were made by Dr A. D. Thackeray with the 74-inch Radcliffe Reflector (scale 1 mm. = 22″·50) and were reduced at the Cape Observatory with the aid of faint reference stars having photographic magnitudes between 11^m and 13^m whose positions had been determined from plates specially taken for this purpose with the Cape Refractors. The Radcliffe exposures were also guided on the stars. The images of the comet are rather faint and difficult to measure.

When two plates of the comet were available for the same night, one was reduced by the usual dependence method using three stars, the other by standard coordinate computation and the use of four quadrantal stars, the reference stars for the two methods being selected as differently as possible. When one plate only was available for a night, this plate was measured twice, once for each method. On November 17, however, only one reference star near the comet was used.

The positions of the reference stars were taken from the Yale Photographic Zone Catalogues when the comet was north of −30° declination and from unpublished Cape Photographic Zone Catalogues when the comet was south of −30°.

The epoch of observation of all the reference stars is comparatively recent, but as proper motions were available their positions were reduced to the epoch of observation of the comet. The positions given in the Cape Catalogues are already on the FK3 system. Those taken from the Yale Catalogues were reduced to the FK3 system by the small corrections shown in Table II. These quantities were obtained from the differences "GC *minus* Yale" given in the introduction

TABLE II

R.A.	Yale Zones	FK3 − Yale	
h	° °	s	″
13	−20 to −22	−0·008	+0·21
13	−22 to −27	−0·006	+0·17
12	−27 to −30	−0·002	+0·23
7	−22 to −27	−0·006	+0·29
6½	−20 to −22	+0·010	+0·19
6	−14 to −18	0·000	−0·17
6	−10 to −14	−0·004	−0·28
6	− 6 to −10	−0·009	+0·30
6	− 2 to − 6	−0·019	+0·39
6	− 2 to + 1	−0·086	+0·21

of the various Yale Catalogues together with the differences " FK3 *minus* GC " as given in the G.C. and also by Kopff in *A.N.*, **269**, 3, 1939.

The estimated magnitudes are based on a graphical smoothing of 40 direct estimates (to the nearest half magnitude) made between 1948 November 8 and 1949 March 30. An investigation of the empirical relation between the observed magnitude (m) and distances (r, Δ) of the comet yielded the following result:—

$$m = 6{\cdot}97 + 5{\cdot}76 \times 2{\cdot}5 \log r + 5 \log \Delta,$$

so that the magnitude of the comet when at unit distance from both Sun and Earth was 7·0, and varied approximately as the sixth power of its inverse distance from the Sun. The exponent given, 5·76, is an average over the range from $r = 0{\cdot}5$ to $r = 3{\cdot}0$. Its actual value varied from 6·3 at $r = 0{\cdot}5$ to 5·4 at $r = 3{\cdot}0$.

Royal Observatory,
Cape of Good Hope:
1949 May 14.

THE EXPANSION OF AN INTERSTELLAR GAS-CLOUD INTO A VACUUM*

G. C. McVittie

(Received 1950 January 30)

Summary

Riemann's work is summarized for the case of the adiabatic one-dimensional motion of an interstellar gas-cloud expanding into a vacuum. Boundary conditions are found for: (A) a homogeneous (isothermal) gas-cloud; (B) a non-homogeneous cloud having a temperature-gradient perpendicular to the face advancing into the vacuum. Due to the asymmetry of the boundary conditions, it is not possible to prove that one of the Riemann variables, s, is constant in case (A). General solution of the problem for case (A) under assumption that s is constant and relation to Burgers' particular solution. Demonstration that atoms of the gas at the advancing face must be given an initial impulsive velocity in case (A). General solution for case (B), in which neither Riemann variable is constant. Advancing face shown to be permanently the seat of "shock" conditions. Method of fitting the solution to any law of temperature-variation in the cloud given *a priori*. Particular example worked out in detail which suggests that Burgers' high speed of advance of the face into the vacuum is attainable only after an infinite time.

We consider a gas-cloud with an infinite plane face, the cloud extending to infinity to the left of the face whilst to the right there is a vacuum. The gas-cloud consists of monatomic hydrogen so that the ratio of specific heats, k, is $\frac{5}{3}$. The equation of state is $p=(R/m)\rho T$ and the temperature of the gas is about 10,000 deg. K. The motion is one-dimensional and the x-axis is taken perpendicular to the face. Adiabatic conditions hold throughout the motion so that $p=\kappa\rho^k$ and there is no viscosity, heat-conduction, radiation pressure, etc. A solution of the problem under these conditions has been given for a homogeneous gas-cloud by Burgers†, who arrives at the somewhat surprising conclusion that the face of the cloud advances into the vacuum with three times the speed of sound in the undisturbed gas. This is about 35 km./sec., which we may compare with the peculiar velocities of some 15 to 20 km./sec. of the clouds themselves. The object of the present investigation is to show that the problem is much more complex than Burgers' treatment would suggest, and to indicate alternative methods of tackling it.

1. *General Theory.*—The fundamental equations governing one-dimensional supersonic flow may not be generally familiar to astronomers and we therefore summarize in this section Riemann's‡ basic investigation of this problem.

* A summary of this paper was read at a Joint Colloquium on Problems of Motion of Gaseous Masses of Cosmical Dimensions, Paris, 1949 August.

† J. M. Burgers, *K. Ned. Akad. v. Wet.*, **49**, 2, Section 2, 1946. The physical data on interstellar gas-clouds are summarized in Section 1 of this paper. See also J. H. Oort, *M.N.*, **106**, 159, 1946, and W. S. Adams, *P.A.S.P.*, **60**, 174, 1948.

‡ B. Riemann, *Oeuvres Mathematiques*, Paris, p. 177, 1898.

The equations of motion and of continuity in the usual notation of hydrodynamics are

$$\frac{\partial u}{\partial t}+u\frac{\partial u}{\partial x}=-\frac{1}{\rho}\frac{\partial p}{\partial x},$$

$$\frac{1}{\rho}\frac{\partial \rho}{\partial t}+\frac{u}{\rho}\frac{\partial \rho}{\partial x}+\frac{\partial u}{\partial x}=0.$$

If the adiabatic condition holds, we can replace ρ by the velocity of sound c, where $c^2=kp/\rho=k\kappa\rho^{k-1}=k(R/m)T$, and the equations become

$$\frac{\partial u}{\partial t}+u\frac{\partial u}{\partial x}+\frac{2c}{k-1}\frac{\partial c}{\partial x}=0, \tag{1.1}$$

$$\frac{2}{k-1}\frac{\partial c}{\partial t}+\frac{2u}{k-1}\frac{\partial c}{\partial x}+c\frac{\partial u}{\partial x}=0. \tag{1.2}$$

The Riemann variables r, s, where

$$\left.\begin{aligned} 2r&=\frac{2c}{k-1}+u,\\ 2s&=\frac{2c}{k-1}-u,\end{aligned}\right\} \quad \text{or} \quad \left\{\begin{aligned} r+s&=\frac{2c}{k-1}, &(1.3)\\ r-s&=u, &(1.4)\end{aligned}\right.$$

transform (1.1), (1.2) into

$$\frac{\partial r}{\partial t}+(u+c)\frac{\partial r}{\partial x}=0, \tag{1.5}$$

$$\frac{\partial s}{\partial t}+(u-c)\frac{\partial s}{\partial x}=0. \tag{1.6}$$

But by (1.3), (1.4)

$$u+c=\alpha r+\beta s, \qquad u-c=-\beta r-\alpha s, \tag{1.7}$$

where

$$\left.\begin{aligned}\alpha&=\tfrac{1}{2}(k+1)\\ \beta&=\tfrac{1}{2}(k-3)\end{aligned}\right\} \quad \text{or} \quad \left.\begin{aligned}\alpha+\beta&=k-1\\ \alpha-\beta&=2.\end{aligned}\right\} \tag{1.8}$$

Hence (1.5), (1.6) become

$$\frac{\partial r}{\partial t}+(\alpha r+\beta s)\frac{\partial r}{\partial x}=0, \tag{1.9}$$

$$\frac{\partial s}{\partial t}-(\beta r+\alpha s)\frac{\partial s}{\partial x}=0. \tag{1.10}$$

It has been shown by Riemann* that, when

$$\frac{\partial r}{\partial x}\frac{\partial s}{\partial x}\neq 0,$$

we can transform to r, s as independent variables. In fact, since

$$dr=\frac{\partial r}{\partial t}dt+\frac{\partial r}{\partial x}dx, \qquad ds=\frac{\partial s}{\partial t}dt+\frac{\partial s}{\partial x}dx,$$

* B. Riemann, *loc. cit.*

we have by (1.9), (1.10),

$$dr = \frac{\partial r}{\partial x}\{-(\alpha r+\beta s)\,dt+dx\} = \frac{\partial r}{\partial x}\{d(x-(\alpha r+\beta s)t)+t(\alpha\,dr+\beta\,ds)\},$$

and similarly

$$ds = \frac{\partial s}{\partial x}\{d(x+(\beta r+\alpha s)t)-t(\beta\,dr+\alpha\,ds)\}.$$

Hence if we write

$$X = x-(\alpha r+\beta s)t, \qquad Y = x+(\beta r+\alpha s)t, \tag{1.11}$$

and regard X, Y as functions of r, s, we have

$$dr = \frac{\partial r}{\partial x}\left\{\left(\frac{\partial X}{\partial r}+\alpha t\right)dr+\left(\frac{\partial X}{\partial s}+\beta t\right)ds\right\},$$

$$ds = \frac{\partial s}{\partial x}\left\{\left(\frac{\partial Y}{\partial r}-\beta t\right)dr+\left(\frac{\partial Y}{\partial s}-\alpha t\right)ds\right\}.$$

But r, s are independent variables, so that the last two equations give

$$\frac{\partial X}{\partial s}+\beta t = 0, \qquad \frac{\partial Y}{\partial r}-\beta t = 0 \tag{1.12}$$

and

$$\frac{\partial r}{\partial x} = \left(\frac{\partial X}{\partial r}+\alpha t\right)^{-1}, \qquad \frac{\partial s}{\partial x} = \left(\frac{\partial Y}{\partial s}-\alpha t\right)^{-1}. \tag{1.13}$$

Since, by (1.12), we have $\partial X/\partial s-(-\partial Y/\partial r)=0$, we can define the total derivative of a function $w(r,s)$ by

$$dw = X\,dr-Y\,ds \tag{1.14}$$

or, using suffixes to denote the partial derivatives of w,

$$\left.\begin{aligned} w_s &= -Y = -x-(\beta r+\alpha s)t,\\ w_r &= X = x-(\alpha r+\beta s)t. \end{aligned}\right\} \tag{1.15}$$

The equations (1.12) and (1.15) yield

$$w_{rs} = -\frac{\partial Y}{\partial r} = -\beta t \tag{1.16}$$

and

$$Y-X = (\alpha+\beta)(r+s)t,$$

or

$$t = -\frac{1}{\alpha+\beta}\,\frac{1}{r+s}\,(w_r+w_s).$$

Hence

$$w_{rs}+\frac{n}{r+s}\,(w_r+w_s) = 0, \tag{1.17}$$

where

$$n = -\frac{\beta}{\alpha+\beta} = \frac{3-k}{2(k-1)}. \tag{1.18}$$

For an arbitrary gas, n may have a non-integral value, but for a monatomic gas $n=1$, a result with important consequences, as we shall see in Section 5.

The analysis leading up to (1.17) presupposes that both $\partial r/\partial x$ and $\partial s/\partial x$ are not zero. If one or other of them is zero, it is best not to introduce the function w but to solve the equations (1.9) and (1.10) directly. We note also that the analysis breaks down when either or both of $\partial r/\partial x$, $\partial s/\partial x$ is infinite. Regions in which this happens we shall describe as being the seat of "shock" conditions: in them the equation $p=\kappa\rho^k$ no longer holds good.

2. *Boundary Conditions.*—Suppose that initially the face of the gas was at $(B_1)_i$, where $x=(x_1)_i$, and that at a later time it is at B_1 and that B_1 is then advancing to the right (see Fig. 1) with speed v_1. The cloud then lies to the left of B_1 whilst

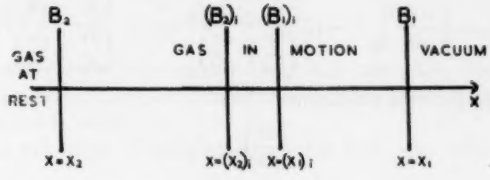

FIG. 1.

to the right of this plane there is a vacuum. Following Burgers, we define B_1 as a plane on which the density of the gas is zero, i.e. by (1.3)

$$r_1+s_1=0. \tag{2.1}$$

The speed of advance of B_1 is $v_1=(dx/dt)_1$, where, by total differentiation of (2.1),

$$\left(\frac{\partial r}{\partial t}+\frac{\partial s}{\partial t}\right)_1+\left(\frac{\partial r}{\partial x}+\frac{\partial s}{\partial x}\right)_1\left(\frac{dx}{dt}\right)_1=0.$$

Using (1.5), (1.6) with $u=u_1$, $c=0$, we obtain

$$v_1=u_1\frac{\left(\dfrac{\partial r}{\partial x}+\dfrac{\partial s}{\partial x}\right)_1}{\left(\dfrac{\partial r}{\partial x}+\dfrac{\partial s}{\partial x}\right)_1}=u_1, \tag{2.2}$$

whether one or other of $(\partial r/\partial x)_1$, $(\partial s/\partial x)_1$ *is zero or not.* Thus the boundary B_1 advances with the speed of the gas at B_1, as it should do.

Strictly speaking (2.1) is the only boundary condition, for we do not know how the expansion started, nor do we know how the successive layers of gas are set in motion as time progresses. However, it is reasonable to suppose that all the gas does not start moving at once and that there is an inner boundary, B_2, to the moving part of the gas. To the left of B_2 the gas is at rest and the pressure and density are continuous from one side of B_2 to the other. Initially B_2 is at $(B_2)_i$, where $x=(x_2)_i$, but we do not for the moment commit ourselves to the statement that $(B_1)_i=(B_2)_i$. The conditions at B_2 are $u_2=0$, $c_2=-c_0$ or by (1.3), (1.4),

$$r_2-s_2=0, \tag{2.3}$$

$$r_2+s_2=-2c_0/(k-1). \tag{2.4}$$

Case (*A*). *Homogeneous* (*isothermal*) *cloud.*—In such a cloud c_0 is a constant. Let B_2 be at x_2 at time t_2 and at x_2-dx at time t_2+dt. Then the speed of advance of B_2 is $v_2=(-dx/dt)_2$, where, by total differentiation of (2.3), (2.4),

$$\left(\frac{\partial r}{\partial t}-\frac{\partial s}{\partial t}\right)_2+\left(\frac{\partial r}{\partial x}-\frac{\partial s}{\partial x}\right)_2\left(\frac{-dx}{dt}\right)_2=0,$$

$$\left(\frac{\partial r}{\partial t}+\frac{\partial s}{\partial t}\right)_2+\left(\frac{\partial r}{\partial x}+\frac{\partial s}{\partial x}\right)_2\left(\frac{-dx}{dt}\right)_2=0.$$

Using (1.5), (1.6) with $u=0$, $c=-c_0$, we have

$$v_2=\left(\frac{-dx}{dt}\right)_2=-c_0\frac{\left(\frac{\partial r}{\partial x}+\frac{\partial s}{\partial x}\right)_2}{\left(\frac{\partial r}{\partial x}-\frac{\partial s}{\partial x}\right)_2}=-c_0\frac{\left(\frac{\partial r}{\partial x}-\frac{\partial s}{\partial x}\right)_2}{\left(\frac{\partial r}{\partial x}+\frac{\partial s}{\partial x}\right)_2}, \tag{2.5}$$

whence we obtain the two conditions

$$\left(\frac{\partial s}{\partial x}\right)_2=0, \tag{2.6}$$

$$v_2=-c_0. \tag{2.7}$$

Hence B_2 moves to the left with the speed of sound in the undisturbed gas. As to the solution of (1.9), (1.10) which will give the motion in the region from B_2 to B_1, all we can say is this:—Let $(B_2)_i$ be the initial position of B_2. Then

$$\left(\frac{\partial s}{\partial x}\right)_2=0$$

at each value of x lying between $(x_2)_i$ and x_2 and so s is constant for such values of x. But this gives us no clue as to the way s varies for values of x between $(x_2)_i$ and x_1 even if initially $(x_2)_i=(x_1)_i$. No doubt we can assert that s is constant for the whole range x_1 to x_2 on the basis of some *additional* assumption, e. g. that s is an analytic function of x. At any rate the boundary conditions alone are insufficient for the purpose and this arises from their asymmetrical character. Had, for example, B_1 been advancing into the same gas at rest, it would have been easy to show that s was constant in the region from $(B_1)_i$ to B_1 also, but this is not the case in our problem.

Case (*B*). *Non-homogeneous cloud.*—We shall now show that the conditions (2.6), (2.7) depend on the postulated homogeneity of the cloud. Let us suppose that the cloud is non-homogeneous in such a way that $c_0=c_0(x)$ is a function of x given *a priori* and valid for that portion of the cloud which, at each instant, has not yet begun to move. We can interpret this condition physically by saying that there is a temperature-gradient in the cloud in a direction perpendicular to the face. We write c_0' for dc_0/dx and differentiate (2.3), (2.4) totally again. We find

$$\left(\frac{\partial r}{\partial t}-\frac{\partial s}{\partial t}\right)_2+\left(\frac{\partial r}{\partial x}-\frac{\partial s}{\partial x}\right)_2\left(\frac{-dx}{dt}\right)_2=0,$$

$$\left(\frac{\partial r}{\partial t}+\frac{\partial s}{\partial t}\right)_2+\left(\frac{\partial r}{\partial x}+\frac{\partial s}{\partial x}\right)_2\left(\frac{-dx}{dt}\right)_2=-\frac{2}{k-1}\left(\frac{-dx}{dt}c_0'\right)_2,$$

whence

$$v_2=\left(\frac{-dx}{dt}\right)_2=-\left\{c_0\frac{\frac{\partial r}{\partial x}+\frac{\partial s}{\partial x}}{\frac{\partial r}{\partial x}-\frac{\partial s}{\partial x}}\right\}_2=\left\{-c_0\frac{\frac{\partial r}{\partial x}-\frac{\partial s}{\partial x}}{\frac{\partial r}{\partial x}+\frac{\partial s}{\partial x}+\frac{2c_0'}{k-1}}\right\}_2.$$

Thus we now have instead of (2.6), (2.7)

$$2\left(\frac{\partial r}{\partial x}\frac{\partial s}{\partial x}\right)_2 = -\frac{1}{k-1}\left\{c_0'\left(\frac{\partial r}{\partial x}+\frac{\partial s}{\partial x}\right)\right\}_2, \tag{2.8}$$

$$v_2 = -\left\{c_0\frac{\frac{\partial r}{\partial x}+\frac{\partial s}{\partial x}}{\frac{\partial r}{\partial x}-\frac{\partial s}{\partial x}}\right\}_2. \tag{2.9}$$

We see at once that a solution of (1.9), (1.10) with

$$\frac{\partial r}{\partial x}=0 \quad \text{or} \quad \frac{\partial s}{\partial x}=0$$

will not do for this case, whatever may happen in case (A). Moreover the non-linearity of the equations does not permit us to argue *a priori* that the motions will possess any feature in common.

3. *Boundary conditions in terms of derivatives of* w.—In cases where

$$\frac{\partial r}{\partial x}\frac{\partial s}{\partial x}\neq 0$$

it is convenient to express the boundary conditions in terms of the derivatives of w.

At B_1.—Let B_1 be at x_1 at time t_1. Then since $r_1+s_1=0$ at B_1 we can write (1.15) as

$$\left.\begin{aligned}(w_s)_1 &= -x_1-(\beta-\alpha)r_1t_1,\\ (w_r)_1 &= x_1+(\beta-\alpha)r_1t_1.\end{aligned}\right\} \tag{3.1}$$

Hence at B_1

$$(w_r+w_s)_1=0. \tag{3.2}$$

This condition being fulfilled, the speed of advance of B_1 is by (2.2), (2.1), (1.4), $v_1=u_1=2r_1$. Hence (3.1), (1.8) yield

$$(w_r)_1=x_1-v_1t_1, \tag{3.3}$$

which is the equation for v_1 in terms of x_1, t_1.

At B_2.—Here $r_2=s_2$ and so (1.15) now becomes

$$\left.\begin{aligned}(w_s)_2 &= -x_2-(\alpha+\beta)r_2t_2,\\ (w_r)_2 &= x_2-(\alpha+\beta)r_2t_2.\end{aligned}\right\} \tag{3.4}$$

Thus there is no condition analogous to (3.2) at B_2 except at the peculiar instant $t_2=0$, which can always be avoided by changing the origin of time. Assuming that this has been done, we may solve (3.4), to give

$$\left.\begin{aligned}x_2 &= \tfrac{1}{2}(w_r-w_s)_2,\\ t_2 &= -\frac{1}{2}\frac{1}{\alpha+\beta}\frac{1}{r_2}(w_r+w_s)_2.\end{aligned}\right\} \tag{3.5}$$

But $r_2=s_2=-c_0(x_2)/(k-1)$ and $\alpha+\beta=k-1$ and therefore the last two equations give

$$\frac{x_2}{t_2}=c_0(x_2)\left\{\frac{w_r-w_s}{w_r+w_s}\right\}_2. \tag{3.6}$$

Again, (1.13), (1.15) and (1.16) yield

$$\frac{\partial r}{\partial x} = \left(w_{rr} - \frac{\alpha}{\beta} w_{rs}\right)^{-1}, \qquad \frac{\partial s}{\partial x} = -\left(w_{ss} - \frac{\alpha}{\beta} w_{rs}\right)^{-1}. \tag{3.7}$$

Hence in case (B) of the preceding section the boundary condition (2.8) becomes

$$2(k-1) = \{c_0'(w_{ss} - w_{rr})\}_2, \tag{3.8}$$

provided however that

$$(w_{rr})_2 \neq \frac{\alpha}{\beta}(w_{rs})_2, \qquad (w_{ss})_2 \neq \frac{\alpha}{\beta}(w_{rs})_2. \tag{3.9}$$

Lastly the formula (2.9) for the rate of advance of B_2 becomes

$$v_2 = -\left\{ c_0 \frac{w_{ss} - w_{rr}}{w_{ss} + w_{rr} - \dfrac{2\alpha}{\beta} w_{rs}} \right\}_2. \tag{3.10}$$

4. *The solution s = constant for case (A).*—We now enquire how far the particular solution of (1.9), (1.10) for which $s = constant$ will fit this case. We can solve the equations for any value of k and therefore we shall not introduce the value $k = \frac{5}{3}$ in our formulae. The equation (1.10) is satisfied identically whilst the constant value of s is determined by the boundary conditions at B_2 (equations (2.3) and (2.4)) to be

$$s = -c_0/(k-1). \tag{4.1}$$

Combining this with the boundary conditions at B_1 (equations (2.1) and (2.2)) and using also (1.4), we obtain

$$v_1 = u_1 = 2r_1 = -2s_1 = 2c_0/(k-1) \tag{4.2}$$

for the rate of advance of B_1. The equation (1.9) is now

$$\frac{\partial r}{\partial t} + \left(\alpha r - \frac{\beta c_0}{k-1}\right)\frac{\partial r}{\partial x} = 0,$$

and its solution is

$$x - t\left(\alpha r - \frac{\beta c_0}{k-1}\right) = f(r), \tag{4.3}$$

where $f(r)$ is an arbitrary function of r. Given this function, the equations (1.3), (1.4) and (4.1) determine u, c in terms of x, t by the simultaneous solution of the equations

$$\left.\begin{aligned} x - t\left\{\tfrac{1}{2}\alpha\left(\frac{2c}{k-1} + u\right) - \frac{\beta c_0}{k-1}\right\} &= f\left(\frac{c}{k-1} + \tfrac{1}{2}u\right), \\ -\frac{2c_0}{k-1} &= \frac{2c}{k-1} - u. \end{aligned}\right\} \tag{4.4}$$

The rate of advance of B_2 has already been found to be $-c_0$ (equation (2.7)). Lastly we obtain by partial differentiation of (4.3), with respect to x,

$$\frac{\partial r}{\partial x} = \left(\alpha t + \frac{\partial f}{\partial r}\right)^{-1} \equiv (\alpha t + f'(r))^{-1}. \tag{4.5}$$

It is easily verified that Burgers' solution * of the problem is obtained by putting $f \equiv 0$ in (4.3), (4.4), his values for u, c being

$$\left.\begin{aligned} u &= \frac{2}{k+1}\left(\frac{x}{t}+c_0\right), \\ \frac{c}{k-1} &= \frac{1}{k+1}\left(\frac{x}{t}-\frac{2c_0}{k-1}\right). \end{aligned}\right\} \tag{4.6}$$

But his results, that the face B_1 advances to the right with speed $2c_0/(k-1)$ whilst B_2 advances to the left with speed c_0, do not depend on these particular expressions for u, c: they are valid for any u, c which satisfy (4.4). Our formulae differ from his in the values assigned to (x_1, t_1) and (x_2, t_2) which Burgers denotes by (x', t') and (x'', t''), respectively. Using (4.4) with $c=0$, $u=u_1=2c_0/(k-1)$, we find

$$x_1 - \frac{2c_0}{k-1}t_1 = f\left(\frac{c_0}{k-1}\right), \tag{4.7}$$

whilst (4.4) with $u=0$, $c=-c_0$ gives

$$x_2 + c_0 t_2 = f\left(-\frac{c_0}{k-1}\right), \tag{4.8}$$

which replace Burgers' $(x/t)' = 2c_0/(k-1)$ and $(x/t)'' = -c_0$, respectively.

We now consider the initial instant, t_i, of the expansion and we denote all initial values by the suffix i. Equations (4.2), (2.3), (2.4) give

$$(r_1)_i = (-s_1)_i = (\tfrac{1}{2}u_1)_i = (\tfrac{1}{2}v_1)_i = c_0/(k-1), \tag{4.9}$$

$$(r_2)_i = (s_2)_i = -c_0/(k-1) \quad \text{and} \quad (u_2)_i = 0. \tag{4.10}$$

The obvious way—though probably not the only conceivable one—of defining the initial instant of the expansion is by the coincidence of $(B_1)_i$ and $(B_2)_i$ in Fig. 1. This means that $(x_1)_i = (x_2)_i$ for $t_i = (t_1)_i = (t_2)_i$, whence from (4.7) and (4.8)

$$\frac{k+1}{k-1}c_0 t_i = -\left\{f\left(\frac{c_0}{k-1}\right) - f\left(-\frac{c_0}{k-1}\right)\right\}, \tag{4.11}$$

$$(x_1)_i = (x_2)_i = \frac{k-1}{k+1}f\left(\frac{c_0}{k-1}\right) + \frac{2}{k+1}f\left(-\frac{c_0}{k-1}\right). \tag{4.12}$$

Also by (4.5), (4.11) we have

$$\left(\left(\frac{\partial r}{\partial x}\right)_1\right)_i = \left[f'\left(\frac{c_0}{k-1}\right) - \frac{k-1}{2c_0}\left\{f\left(\frac{c_0}{k-1}\right) - f\left(-\frac{c_0}{k-1}\right)\right\}\right]^{-1}, \tag{4.13}$$

$$\left(\left(\frac{\partial r}{\partial x}\right)_2\right)_i = \left[f'\left(-\frac{c_0}{k-1}\right) - \frac{k-1}{2c_0}\left\{f\left(\frac{c_0}{k-1}\right) - f\left(-\frac{c_0}{k-1}\right)\right\}\right]^{-1}. \tag{4.14}$$

Now consider Burgers' solution in which $f \equiv 0$. By (4.11), (4.12) this implies that

$$t_i = 0, \qquad (x_1)_i = (x_2)_i = 0,$$

and, by (4.13), (4.14), that

$$\left(\left(\frac{\partial r}{\partial x}\right)_1\right)_i = \left(\left(\frac{\partial r}{\partial x}\right)_2\right)_i = \infty.$$

Hence at the commencement of the motion we have two features worthy of comment, viz.: (i) the face of the cloud is the seat of "shock" conditions, and (ii) the initial

* J. M. Burgers, *loc. cit.*

outward speed of the face is $2c_0/(k-1)$. As Burgers himself remarks, such an initial state is somewhat artificial. The condition (i) survives even if we use the solution (4.3) instead of Burgers'. For, since f is arbitrary, we may limit it by choosing $t_i=0$ in (4.11) and this then means that f is an even function of r. Thus f' is an odd function of r and therefore the two values of $\partial r/\partial x$ given by (4.13), (4.14) respectively are either different, which is impossible, or singular, which again makes the face of the cloud the seat of "shock" conditions at the initial instant. It is perhaps not relevant in a hydrodynamical treatment to introduce a consideration drawn from the kinetic theory of gases. However, we may remark that, if V is the root mean square velocity of the atoms of the gas when its temperature is T, then $V^2=3(R/m)T$, whilst the speed of sound is related to T by $c^2=k(R/m)T$. Thus when $k=\frac{5}{3}$ we have $c^2=5V^2/9$ which combined with (4.9) gives $(u_1)_i=3c_0=\sqrt{5}V$. Hence the initial speed of the gas at the face is $\sqrt{5}$ times the root mean square velocity of the atoms, whereas, in the absence of an impulsive force at the face, we should not expect the initial speed to exceed V. Our general conclusion is that this difficulty, as well as the high speed of advance of the face ($3c_0$ for a monatomic gas), is due to the assumption $s=$ *constant* which, as we have seen, we are not compelled to make by the conditions of the problem.

5. *The general solution for case* (*B*).—In this problem we have to use a solution of (1.9), (1.10) for which both $\partial r/\partial x$ and $\partial s/\partial x$ are different from zero, which we find by solving (1.17). The integration of this equation for an arbitrary value of n requires the use of Riemann's method *, but for our monatomic gas $n=1$ and we can employ the simpler method of Laplace.† We write (1.17) in the equivalent form

$$\frac{\partial}{\partial r}\left\{\frac{\partial w}{\partial s}+\frac{w}{r+s}\right\}+\frac{1}{r+s}\left\{\frac{\partial w}{\partial s}+\frac{w}{r+s}\right\}=0,$$

the integration of which reduces to the successive integration of the two equations

$$\frac{\partial W}{\partial r}+\frac{W}{r+s}=0, \tag{5.1}$$

$$\frac{\partial w}{\partial s}+\frac{w}{r+s}=W. \tag{5.2}$$

From (5.1) we obtain $W=F(s)/(r+s)$, where $F(s)$ is an arbitrary function of s, and then (5.2) gives the general integral of (1.17), viz.

$$w=\frac{S(s)+R(r)}{r+s}, \tag{5.3}$$

where $R(r)$ is an arbitrary function of r and $S(s)=\int F(s)\,ds$. Writing $S'=dS/ds$, $R'=dR/dr$, etc., the various partial derivatives of w are

$$\left.\begin{aligned} w_r&=\frac{R'(r)}{r+s}-\frac{S(s)+R(r)}{(r+s)^2}, & w_s&=\frac{S'(s)}{r+s}-\frac{S(s)+R(r)}{(r+s)^2},\\ w_{rr}&=\frac{R''}{r+s}-\frac{2R'}{(r+s)^2}+\frac{2(S+R)}{(r+s)^3}, & w_{ss}&=\frac{S''}{r+s}-\frac{2S'}{(r+s)^2}+\frac{2(S+R)}{(r+s)^3},\\ w_{rs}&=-\frac{S'+R'}{(r+s)^2}+\frac{2(S+R)}{(r+s)^3}. \end{aligned}\right\} \tag{5.4}$$

* G. Darboux, *Leçons sur la Théorie Générale des Surfaces*, Paris, Vol. II, chap. IV, 1915.
† G. Darboux, *loc. cit.*, chap. II.

The equations for r, s (and so for u, c) in terms of x, t are, by (1.15), (5.4),

$$\left.\begin{aligned} -x-(\beta r+\alpha s)t &= \frac{S'}{r+s}-\frac{S+R}{(r+s)^2}, \\ x-(\alpha r+\beta s)t &= \frac{R'}{r+s}-\frac{S+R}{(r+s)^2}, \end{aligned}\right\} \tag{5.5}$$

whilst by (3.7) with $\alpha/\beta=(k+1)/(k-3)=-2$, we have

$$\left.\begin{aligned} \frac{\partial r}{\partial x} &= (r+s)^3[(r+s)^2R''-2(r+s)(S'+2R')+6(S+R)]^{-1}, \\ \frac{\partial s}{\partial x} &= -(r+s)^3[(r+s)^2S''-2(r+s)(2S'+R')+6(S+R)]^{-1}. \end{aligned}\right\} \tag{5.6}$$

We now apply the boundary conditions. At B_1 we have $r_1=-s_1$ and by (3.2), (5.4)

$$\left[\frac{R'(r)+S'(s)}{r+s}-\frac{2(S+R)}{(r+s)^2}\right]_1=0. \tag{5.7}$$

Suppose that $R(r)$, $S(s)$ are functions having Taylor expansions in the region between B_1 and B_2. Consider a plane B_1' for which $r+s=\epsilon$, where ϵ is small. Then $B_1'\to B_1$ as $\epsilon\to 0$ and $r\to r_1$ and we can write (5.7) in the form

$$\operatorname*{Lim}_{\substack{\epsilon\to 0\\ r\to r_1}}\frac{1}{\epsilon^2}\left[-2\{S(-r)+R(r)\}+\epsilon\{R'(r)-S'(-r)\}+\frac{\epsilon^3}{6}S'''(-r)+O(\epsilon^4)\right]=0.$$

For this limit to exist we must have

$$R(r_1)+S(-r_1)=0, \qquad R'(r_1)-S'(-r_1)=0.$$

But the first of these conditions implies the second, provided that

$$S(s)=-R(-s), \tag{5.8}$$

and, of course, $R'(-s)$ now means $dR(-s)/d(-s)=-dR(-s)/ds$. If now we calculate the values of $\partial r/\partial x$, $\partial s/\partial x$ at B_1, using (5.6), (5.8) and the same limiting process, we find

$$\left.\begin{aligned} \left(\frac{\partial r}{\partial x}\right)_1 &= \operatorname*{Lim}_{\substack{\epsilon\to 0\\ r\to r_1}}\epsilon^3\left[+\frac{\epsilon^4}{12}R^{\mathrm{IV}}(r)+O(\epsilon^5)\right]^{-1}, \\ \left(\frac{\partial s}{\partial x}\right)_1 &= \operatorname*{Lim}_{\substack{\epsilon\to 0\\ r\to r_1}}\epsilon^3\left[+\frac{\epsilon^4}{12}R^{\mathrm{IV}}(r)+O(\epsilon^5)\right]^{-1}. \end{aligned}\right\} \tag{5.9}$$

Hence both $(\partial r/\partial x)$, $(\partial s/\partial x)$ have infinite values at B_1 which is therefore the seat of "shock" conditions throughout the motion. At B_1' the two equations (5.5) become, in virtue of (5.8),

$$\begin{aligned} x-(2r-\alpha\epsilon)t &= \tfrac{1}{2}R''(r)+O(\epsilon), \\ x-(2r+\beta\epsilon)t &= \tfrac{1}{2}R''(r)+O(\epsilon). \end{aligned}$$

Thus at B_1, where $\epsilon = 0$ and $r_1 = \frac{1}{2}u_1 = \frac{1}{2}v_1$ *, we obtain, using also (1.8), the single equation

$$x_1 - v_1 t_1 = \tfrac{1}{2}R''(\tfrac{1}{2}v_1), \tag{5.10}$$

which gives the speed of advance of B_1 in terms of x_1, t_1.

We next turn to B_2, where $r_2 = s_2 = -\frac{3}{2}c_0(x_2)$. It is simpler to work in terms of r_2 rather than of $c_0(x_2)$ and we shall also use for brevity the notation

$$\left.\begin{aligned} R(r_2) &= R_+, \qquad R'(r_2) = R'_+, \text{ etc.,} \\ R(-r_2) &= R_-, \qquad R'(-r_2) = R'_- \text{ etc.} \end{aligned}\right\} \tag{5.11}$$

Firstly, we can obtain the position of B_2 at any time by (3.5), (5.4), (5.8),

$$\left.\begin{aligned} x_2 &= \frac{1}{4}\frac{1}{r_2}(R'_+ - R'_-), \\ t_2 &= \frac{3}{8}\frac{1}{r_2^3}\{-r_2(R'_+ + R'_-) + (R_+ - R_-)\}. \end{aligned}\right\} \tag{5.12}$$

We shall see in a moment that the first of these equations is equivalent to a relation between the functions R and c_0. It is the second which then gives x_2 as a function of t_2 and so fixes the position of B_2 at each instant. Secondly, we can find the speed of B_2 by (3.10), (5.4), (5.8) and the fact that $c_0 = -\frac{3}{8}r_2$, viz.

$$v_2 = \tfrac{8}{3}r_2^2 \frac{R'_+ - R'_- - r_2(R''_+ + R''_-)}{3(R_+ - R_-) - 3r_2(R'_+ + R'_-) + r_2^2(R''_+ - R''_-)}. \tag{5.13}$$

Thirdly, we can show as follows that the boundary condition (2.8) in its form (3.8) enables us to find the functional form of R when we are given the function $c_0(x_2)$. We have by (3.8), (5.4),

$$1 = \frac{1}{4}\frac{1}{r_2^2}\frac{dr_2}{dx_2}\{-R'_+ + R'_- + r_2(R''_+ + R''_-)\}.$$

Using (5.11) this may be written

$$1 = \frac{1}{4}\frac{dr_2}{dx_2}\frac{d}{dr_2}\left[\frac{1}{r_2}\frac{d}{dr_2}\{R(r_2) + R(-r_2)\}\right],$$

which on integration yields the first of the equations (5.12), viz.

$$x_2 = \frac{1}{4}\frac{1}{r_2}\frac{d}{dr_2}\{R(r_2) + R(-r_2)\} = \frac{1}{4}\frac{1}{r_2}(R'_+ - R'_-).$$

But now $r_2 = -\frac{3}{2}c_0(x_2)$ is a (known) function of x_2, so that the last equation becomes

$$4x_2 r_2 r_2' = \frac{d}{dx_2}\{R(r_2) + R(-r_2)\},$$

---

* I am indebted to Professor E. T. Copson, University College, Dundee, for a proof of this statement. We have, if $B_1' \to B_1$, that

$$x_1 - 2r_1 t_1 = \tfrac{1}{2}R''(r_1).$$

Since $v_1 = dx_1/dt_1$ and $u_1 = 2r_1$, we obtain, on differentiating with respect to t_1,

$$v_1 = u_1 + \{2t_1 + \tfrac{1}{2}R'''(r_1)\}(dr_1/dt_1).$$

But by (1.16), (5.4) and (1.8) with $k = \frac{4}{3}$, we have

$$\tfrac{2}{3}t = tc_{rs} = 2\frac{S+R}{(r+s)^3} - \frac{S'+R'}{(r+s)^2},$$

and if in this we put $r = r_1$, $s = -r_1 + \epsilon$, use (5.8) and allow $\epsilon \to 0$, we have $2t_1 + \frac{1}{2}R'''(r_1) = 0$, so that $v_1 = u_1$.

which on integration of the left-hand side by parts yields

$$R(r_2)+R(-r_2)=2\{C+x_2r_2^2-\int r_2^2\,dx_2\}, \tag{5.14}$$

where C is a constant of integration. If c_0^{-1} denotes the function inverse to c_0 we have $x_2=c_0^{-1}(-\frac{2}{3}r_2)$ and therefore we may express the right-hand side of (5.14), after performing the integration in the last term, as an explicit function of r_2. We can then, in principle at least, select the function R which will satisfy (5.14) and thus determine the solution of (1.17) appropriate to the given temperature-distribution in the undisturbed cloud.

We shall not discuss the initial instant of the expansion in this general case as we can illustrate the question more clearly by means of a specific example to which we now proceed.

6. *A particular solution for case* (B).—Let us suppose that initially $(B_2)_i$ is situated *to the left* of the origin of x and that we are given that

$$c_0^2(x)=a^2-\frac{4}{9}\left(\frac{\frac{3}{2}Aa}{-x}\right)^{1/2} \qquad (x<0), \tag{6.1}$$

where A, a are positive constants. Hence

$$r_2^2=\tfrac{9}{4}c_0^2(x_2)=\tfrac{9}{4}a^2-\left(\frac{\frac{3}{2}Aa}{-x_2}\right)^{1/2}$$

or

$$x_2=-\tfrac{3}{2}Aa/(\tfrac{9}{4}a^2-r_2^2)^2. \tag{6.2}$$

With these values (5.14) becomes, after evaluation of the integral and simplification,

$$R(r_2)+R(-r_2)=2\{C-\tfrac{3}{2}Aa/(\tfrac{9}{4}a^2-r_2^2)\}.$$

Without loss of generality we may put C equal to zero and then

$$R(r_2)=-A(\tfrac{3}{2}a-r_2)^{-1}; \qquad R(-r_2)=-A(\tfrac{3}{2}a+r_2)^{-1}$$

satisfy the equation. Hence, using (5.8), (5.3), the solution of (1.17) corresponding to the expression (6.1) for $c_0(x)$ is

$$\left.\begin{aligned} R(r)&=-A(\tfrac{3}{2}a-r)^{-1}, \qquad S(s)=A(\tfrac{3}{2}a+s)^{-1},\\ w&=-A(\tfrac{3}{2}a-r)^{-1}(\tfrac{3}{2}a+s)^{-1},\end{aligned}\right\} \tag{6.3}$$

which implies that

$$\left.\begin{aligned} R_+&=-A(\tfrac{3}{2}a-r_2)^{-1}, \qquad R'_+=-A(\tfrac{3}{2}a-r_2)^{-2}, \qquad R''_+=-2A(\tfrac{3}{2}a-r_2)^{-3},\\ R_-&=-A(\tfrac{3}{2}a+r_2)^{-1}, \qquad R'_-=-A(\tfrac{3}{2}a+r_2)^{-2}, \qquad R''_-=-2A(\tfrac{3}{2}a+r_2)^{-3}.\end{aligned}\right\} \tag{6.4}$$

From these values, together with (6.2), we find that the second of the equations (5.12) becomes

$$(-x_2)/t_2=a, \qquad (t_2>0), \tag{6.5}$$

which gives the position of B_2 at any instant. Finally (6.4), (5.13) yield

$$v_2=-a, \tag{6.6}$$

which shows that the speed of B_2 is constant throughout the motion. Moreover, by (6.1), this constant is equal to the speed of sound in the far interior of the cloud, i.e. in regions remote from the face advancing into the vacuum.

It is of interest to find the expressions for u, c in the moving part of the cloud in terms of x, t. Using (6.3), equations (5.5) become

$$\left.\begin{aligned} x+(\beta r+\alpha s)t &= -A(\tfrac{3}{2}a-r)^{-1}(\tfrac{3}{2}a+s)^{-2}, \\ x-(\alpha r+\beta s)t &= -A(\tfrac{3}{2}a-r)^{-2}(\tfrac{3}{2}a+s)^{-1}. \end{aligned}\right\} \tag{6.7}$$

If we multiply the first equation by $(\frac{3}{2}a+s)$ and the second by $(\frac{3}{2}a-r)$ we have

$$(\tfrac{3}{2}a+s)\{x+(\beta r+\alpha s)t\} = (\tfrac{3}{2}a-r)\{x-(\alpha r+\beta s)t\},$$

which by (1.4), (1.8) becomes after some re-arrangement

$$(r+s)\{x+(a-\tfrac{4}{3}u)t\} = 0. \tag{6.8}$$

Again, subtracting the two equations (6.7) we obtain

$$(\alpha+\beta)(r+s)t = A(r+s)(\tfrac{3}{2}a-r)^{-2}(\tfrac{3}{2}a+s)^{-2},$$

which by (1.3), (1.4), (1.8) becomes

$$(r+s)[\tfrac{4}{3}t - A\{(\tfrac{1}{2}u-\tfrac{3}{2}a)^2-\tfrac{9}{4}c^2\}^{-2}] = 0. \tag{6.9}$$

We solve these equations by equating the second factors to zero in each case and therefore

$$\left.\begin{aligned} u &= \frac{3}{4}\left(\frac{x}{t}+a\right), \\ c &= \frac{1}{4}\left\{\left(\frac{x}{t}-3a\right)^2 - \frac{64}{9}\left(\frac{\frac{3}{2}A}{t}\right)^{1/2}\right\}^{1/2}. \end{aligned}\right\} \tag{6.10}$$

Comparing these with Burgers' values (4.6) for a homogeneous cloud in which $k=\frac{5}{3}$, we observe that our values approximate in form to Burgers' for large values of t.

Turning now to the determination of the speed and position of the advancing face B_1, we have by (5.10), (6.3)

$$x_1 - v_1 t_1 = -A(\tfrac{3}{2}a-\tfrac{1}{2}v_1)^{-3} = -8A(3a-v_1)^{-3}.$$

If we use the first of the equations (6.10) with $u_1 \equiv v_1$ we have also

$$v_1 = \frac{3}{4}\left(\frac{x_1}{t_1}+a\right). \tag{6.11}$$

A solution of these two equations which, as we shall presently see, corresponds to a physically plausible initial state for the expansion is

$$\left.\begin{aligned} x_1 &= 3at_1 - 4\left(\frac{8A}{27}\right)^{1/4} t_1^{3/4}, \\ v_1 &= 3\left\{a - \left(\frac{8A}{27}\right)^{1/4} t_1^{-1/4}\right\}. \end{aligned}\right\} \tag{6.12}$$

Finally, let us consider the initial instant of the expansion, which we again define by $(B_1)_i = (B_2)_i$ at time t_i. Instead of equations (4.9), (4.10) we have

$$\left.\begin{aligned} (r_1)_i = (-s_1)_i = (\tfrac{1}{2}u_1)_i = (\tfrac{1}{2}v_1)_i &= \tfrac{3}{2}c_i, \\ (r_2)_i = (s_2)_i = -\tfrac{3}{2}c_i, \qquad (u_2)_i &= 0, \end{aligned}\right\} \tag{6.13}$$

where we have written c_i for the value of $c_0(x)$ calculated at the initial position $(x_1)_i=(x_2)_i$. But (6.5) now gives $t_i=(-x_1)_i/a=(-x_2)_i/a$, so that the first of equations (6.10) is

$$(u_1)_i=\frac{3}{4}\left(a+\frac{(x_1)_i}{t_i}\right)=\frac{3}{4}\left(a+\frac{(x_2)_i}{t_i}\right)=0.$$

Hence also, by (6.11), $(v_1)_i=0$ and it therefore follows by (6.13) that $c_i=0$, a result which we can interpret by saying that initially the face of the cloud is at the absolute zero of temperature.* The second of the equations (6.10), (6.12), respectively, when evaluated at the initial instant, are identities, provided that $t_i=8A/(27a^4)$, and by the first of the equations (6.12) we find

$$(x_1)_i=(x_2)_i=-8A/(27a^3).$$

Thus the constant A in the solution (6.3) depends on the initial position of the face of the cloud.

Summarizing the conclusions which we draw from this example, we may say that, if the expansion begins with B_2 coincident with B_1, the face of the cloud is then at the absolute zero of temperature and the motion starts with B_2 moving off to the left at the speed a, whilst B_1 remains momentarily at rest. In common with all the solutions of type (5.3), the advancing face is permanently the seat of "shock" conditions. Moreover (6.12) indicates that the high speed of the advancing face found by Burgers—three times the velocity of sound in the undisturbed gas of a homogeneous cloud—is unlikely to be realized in nature. In our non-homogeneous cloud, with its "cold" initial edge, such a high speed would only be attained as a limit after the expansion had proceeded for an infinite time.

Queen Mary College,
Mile End Road,
London, E.1 :
1950 *January* 29.

* Incidentally we should then also have at the face a zero root mean square velocity which would thus be identical with $(v_1)_i$.

THE EXPANSION OF A GAS CLOUD INTO A VACUUM

E. T. Copson

(Communicated by G. C. McVittie)

(Received 1950 February 17)

Summary

The paper solves by Riemann's method the one-dimensional problem of the expansion of a gas cloud into a vacuum. The cloud is initially at rest, and is homogeneous except for a boundary layer of arbitrary thickness. Motion starts in the non-homogeneous layer, and spreads into the cloud.

The solution uses Riemann's variables $r=\frac{1}{2}(3c+u)$, $s=\frac{1}{2}(3c-u)$, where c is the local velocity of sound, u the gas velocity. In the first stage of the motion there are three moving boundaries. In $x>x_1(t)$, there is a vacuum; in $x_2(t)<x<x_1(t)$, r and s are both variable; in $x_3(t)<x<x_2(t)$, r is constant; in $x<x_3(t)$, the gas is homogeneous and at rest. The boundaries $x=x_1(t)$ and $x=x_2(t)$ move to the right; and, as x_2 increases more rapidly than x_1, the two boundaries coincide at the end of the first stage of the motion. The boundary $x=x_3(t)$ moves into the cloud with the local velocity of sound.

In the second stage of the motion, the quantity r is constant everywhere. The cloud still advances into the vacuum, and the motion spreads as before into the cloud. This state is similar to one discovered by Burgers. The difficulty regarding the discontinuity in the initial state of Burgers' solution is shown to be due to the fact that his solution is a limiting case of the present solution when the thickness of the initial layer of non-homogeneity is made to vanish.

---

1. *Introduction.*—This paper is concerned with the one-dimensional problem of the expansion of a gas cloud into a vacuum. The cloud extends to infinity on one side of its infinite plane face; on the other side of the face there is a vacuum into which the cloud is advancing. It is assumed that the pressure and density satisfy the adiabatic law $p=k\rho^{\gamma}$ everywhere; and the effects of viscosity, heat conduction and radiation are neglected.

The first solution of a problem of this type was obtained by J. M. Burgers.* In this solution, only a layer of the cloud is in motion, the rest being stationary with uniform pressure and density. The boundary between the stationary and moving parts of the cloud moves into the cloud with constant speed a, the velocity of sound in the gas at rest, whereas the face of the cloud advances into the vacuum with speed $2a/(\gamma-1)$. The surprisingly high speed of advance—$3a$ for a cloud of monatomic hydrogen with $\gamma=\frac{5}{3}$—is a somewhat unsatisfactory feature of this solution. A second is that the motion would appear to be due to an unusual type of discontinuity at the face of the cloud at the initial instant when the two moving interfaces coincide and the cloud is at rest.

A second solution has been found by G. C. McVittie† for the case $\gamma=\frac{5}{3}$, by means of Riemann's theory of the propagation of sound waves of finite amplitude.

* J. M. Burgers, *K. Ned. Akad. v. Wet.*, **49**, 588–607, 1946.

† Lecture given at the Joint Colloquium on Problems of Motions of Gaseous Masses of Cosmical Dimensions held at the Institut d'Astrophysique, Paris, 1949 August 16–19. G. C. McVittie, *M.N.*, **110**, 224, 1950.

McVittie's cloud is, in some respects, of the same general type as Burgers'; as the cloud advances into the vacuum, the depth of the layer of gas in motion increases. The speed of advance of the cloud face is, however, no longer constant; Burgers' velocity $3a$ is the terminal velocity of advance of McVittie's cloud.

Despite the elegance of McVittie's solution, it is not a very satisfactory model. He assumes that the stationary part of the cloud is non-homogeneous; but if the adiabatic law held throughout the cloud, this would imply that the whole cloud is in motion. This difficulty can be overcome by assuming that the temperature of the cloud is proportional to ρ^{-1} when the gas is at rest but proportional to $\rho^{\gamma-1}$ when the gas is moving*; but this seems a very artificial solution of the difficulty.

A third type of solution is given in the present paper. The cloud is assumed to be initially at rest and is homogeneous except in a layer of arbitrary depth near the face. This layer starts moving and the face of the cloud advances into the vacuum. But in the cloud there are now two moving boundaries, one moving to the right, the other to the left; between them Riemann's variable r remains constant. After a certain finite time the former boundary catches up the face of the cloud. Thereafter the face of the cloud advances with constant speed $3a$, and Riemann's variable r is everywhere constant; in short, the motion is now very like that in Burgers' model. In the second stage of the motion the difficulty of the high velocity of the face of the cloud remains; but the time taken to reach the second stage can be increased indefinitely by increasing the depth of the initial non-homogeneous layer. The Burgers model, on the other hand, corresponds to the limit as the depth of the initial layer tends to zero, and this explains the difficulty of the initial discontinuity at the face of the cloud.

2. *The equations of motion and the boundary conditions.*—The motion being in one dimension, the dynamical equation is

$$\frac{\partial u}{\partial t} + u\frac{\partial u}{\partial x} = -\frac{1}{\rho}\frac{\partial p}{\partial x}$$

whilst the equation of continuity is

$$\frac{\partial \rho}{\partial t} + u\frac{\partial \rho}{\partial x} + \rho\frac{\partial u}{\partial x} = 0$$

in the usual notation. Since, by hypothesis, the adiabatic condition $p = k\rho^{\gamma}$ is true everywhere, we may replace the variable ρ by the local velocity of sound c defined by the equation

$$c^2 = \frac{dp}{d\rho} = k\gamma\rho^{\gamma-1}.$$

The motion is then governed by the pair of equations

$$\frac{\partial u}{\partial t} + u\frac{\partial u}{\partial x} + \frac{2c}{\gamma-1}\frac{\partial c}{\partial x} = 0, \tag{2.1}$$

$$\frac{2}{\gamma-1}\frac{\partial c}{\partial t} + \frac{2u}{\gamma-1}\frac{\partial c}{\partial x} + c\frac{\partial u}{\partial x} = 0. \tag{2.2}$$

* Professor McVittie made this suggestion to me in a letter. I owe him my hearty thanks for interesting me in this problem and for his valuable criticisms of my work.

If, in the initial state, the gas is at rest but is non-homogeneous, we have $u=0$, $c=c_0(x)$ when $t=0$. Equation (2.1) then gives

$$\left(\frac{\partial u}{\partial t}\right)_0 = -\frac{2}{\gamma-1}c_0(x)c_0'(x),$$

so that the initial acceleration is non-zero, and the cloud starts moving. This shows that McVittie's solution is, as stated in the introduction, incompatible with the adiabatic law. The equation also shows that, if the cloud lies initially in the region $x<h$ say, it is necessary, if expansion occurs, that $c_0'(x)$ be negative at least in some neighbourhood of the face of the cloud. We shall assume that $c_0'(x)$ is negative in the whole layer of initial non-homogeneity.

We shall, moreover, consider only continuous initial states of the cloud, so that when $t=0$, $u=0$ and ρ and c are continuous functions of x. It follows that, in the subsequent motion, shock conditions cannot occur in the cloud. The face of the cloud must, however, be a moving surface of discontinuity. Now if $x=\xi(t)$ is a moving surface of discontinuity, the conditions of conservation of mass, momentum and energy require the continuity of

$$\rho(u-\dot{\xi}), \qquad \rho u(u-\dot{\xi})+p \quad \text{and} \quad \rho(\tfrac{1}{2}u^2+e)(u-\dot{\xi})+pu$$

across the surface, e being the internal energy per unit mass. It follows in the adiabatic case that, since ρ is zero in the vacuum on one side of the face of the cloud, then, in the cloud ρ and c must tend to the limit zero as we move up to the face. No information is obtained concerning the limit of u or the value of $\dot{\xi}$.

3. *Riemann's form of the equations of motion.*—As McVittie has pointed out, it is best in this sort of problem to use Riemann's variables

$$r=\frac{c}{\gamma-1}+\frac{u}{2}, \qquad s=\frac{c}{\gamma-1}-\frac{u}{2}.$$

The equations (2.1) and (2.2) then become

$$\frac{\partial r}{\partial t}+(\alpha r+\beta s)\frac{\partial r}{\partial x}=0, \tag{3.1}$$

$$\frac{\partial s}{\partial t}-(\alpha s+\beta r)\frac{\partial s}{\partial x}=0, \tag{3.2}$$

where $\alpha=\frac{1}{2}(\gamma+1)$, $\beta=\frac{1}{2}(\gamma-3)$.

If one of the variables r, s is a constant, one of these equations is an identity, and the other determines the remaining variable. In the general case the equations can be linearized by taking r and s as independent variables. We then have

$$x-(\alpha r+\beta s)t=\frac{\partial w}{\partial r}, \tag{3.3}$$

$$x+(\alpha s+\beta r)t=-\frac{\partial w}{\partial s}, \tag{3.4}$$

where

$$\frac{\partial^2 w}{\partial r\partial s}-\frac{\beta}{(\alpha+\beta)(r+s)}\left\{\frac{\partial w}{\partial r}+\frac{\partial w}{\partial s}\right\}=0. \tag{3.5}$$

From now on we shall consider only the simplest case in which

$$\gamma=\tfrac{5}{3}, \qquad \alpha=\tfrac{4}{3}, \qquad \beta=-\tfrac{2}{3}.$$

The partial differential equation (3.5) simplifies to

$$\frac{\partial^2 w}{\partial r \partial s} + \frac{1}{(r+s)}\left\{\frac{\partial w}{\partial r} + \frac{\partial w}{\partial s}\right\} = 0,$$

of which the solution is

$$w = \frac{R(r)+S(s)}{r+s},$$

where $R(r)$ and $S(s)$ are arbitrary functions of r and s respectively. Equations (3.1) and (3.2) then give

$$x-(\tfrac{4}{3}r-\tfrac{2}{3}s)t = \frac{R'}{r+s} - \frac{R+S}{(r+s)^2}, \tag{3.6}$$

$$x+(\tfrac{4}{3}s-\tfrac{2}{3}r)t = -\frac{S'}{r+s} + \frac{R+S}{(r+s)^2}, \tag{3.7}$$

where accents denote derivatives with respect to the relevant variables. When R and S have been determined from the initial conditions, these equations will give r and s in terms of x and t.

4. *The initial value problem.*—Let us consider a gas cloud in which the adiabatic law $p=k\rho^{5/3}$ holds everywhere. Initially the cloud is at rest in the region $x \leqslant h$; the region $x>h$ is a vacuum. The portion of the cloud in which $x<0$ is homogeneous, whereas the layer $0 \leqslant x \leqslant h$ is non-homogeneous. The initial conditions are therefore

$$u=0, \qquad c=a \qquad (x<0),$$
$$u=0, \qquad c=c_0(x) \qquad (0 \leqslant x \leqslant h),$$

where, in view of the continuity assumptions made in Section 2, $c_0(0)=a$, $c_0(h)=0$. In terms of the variables r and s, these conditions are

$$r=s=b \qquad (x<0),$$
$$r=s=r_0(x) \qquad (0 \leqslant x \leqslant h),$$

where $$r_0(0)=b, \qquad r_0(h)=0, \qquad b=\tfrac{3}{2}a.$$

We assume, in addition, that $r_0'(x)<0$, so that each particle of the non-homogeneous layer starts to move to the right. At time t the position of the face of the cloud will be $x=x_1(t)$; and on this face $r+s=0$.

It is known from Riemann's work on the propagation of sound waves of finite amplitude that a region in which r is constant moves to the right, whereas one in which s is constant moves to the left. Hence the initial boundary of the non-homogeneous layer will split into two boundaries, and the state at time t will be as follows during the first stage of the motion:—

in the region $x<x_3(t)$, $\quad r=s=b$;
in the region $x_3(t)<x<x_2(t)$, $\quad r=b$, $\quad s=s'(x,t)$;
in the region $x_2(t)<x<x_1(t)$, $\quad r=r(x,t)$, $\quad s=s(x,t)$.

The positions of the two boundaries in the cloud are, *a priori*, unknown; all we are given is that r and s are continuous across the boundaries, so that

$$r(x_2,t)=b, \qquad s(x_2,t)=s'(x_2,t), \qquad s'(x_3,t)=b.$$

We consider first the region $x_2(t)<x<x_1(t)$. When $t=0$, this is the non-homogeneous layer in which $r=s=r_0(x)$. Hence, by (3.6), (3.7),

$$x=\frac{R'(r_0)}{2r_0}-\frac{R(r_0)+S(r_0)}{4r_0^2},$$

$$x=-\frac{S'(r_0)}{2r_0}+\frac{R(r_0)+S(r_0)}{4r_0^2}.$$

Equating the two values of x, we have

$$\frac{R'(r_0)+S'(r_0)}{r_0}-\frac{R(r_0)+S(r_0)}{r_0^2}=0.$$

But as r_0 is an arbitrary function of the variable x, this implies

$$R(r_0)+S(r_0)=2Ar_0,$$

where A is a constant. We may therefore write

$$R(r)=Ar+\phi(r), \qquad S(r)=Ar-\phi(r),$$

and equations (3.6) and (3.7) then become

$$x-(\tfrac{4}{3}r-\tfrac{2}{3}s)t=\frac{\phi'(r)}{r+s}-\frac{\phi(r)-\phi(s)}{(r+s)^2}, \tag{4.1}$$

$$x+(\tfrac{4}{3}s-\tfrac{2}{3}r)t=\frac{\phi'(s)}{r+s}+\frac{\phi(r)-\phi(s)}{(r+s)^2}. \tag{4.2}$$

When $t=0$, either of these equations gives

$$x=\frac{\phi'(r_0)}{2r_0}, \tag{4.3}$$

where $r=r_0(x)$ is the common initial value of r and s. Now, by hypothesis, $r_0(x)$ decreases steadily in $0\leqslant x\leqslant h$, and so has a one-valued inverse function $x(r_0)$, defined in the range $0\leqslant r_0\leqslant b$. It follows that

$$\phi(r_0)=2\int_0^{r_0}rx(r)\,dr.$$

Thus $\phi(r)$ is defined by the initial conditions in the range $0\leqslant r\leqslant b$; we have next to continue the definition to negative values of r. We do this by considering the behaviour of the solution (4.1) and (4.2) as $x\to x_1(t)$.

As $x\to x_1(t)$, $r+s\to 0$. Hence on the face of the cloud,

$$r=r_1(t)=r(x_1,t)>0, \qquad s=s_1(t)=s(x_1,t)<0,$$

where $r_1+s_1=0$. Now, if we subtract (4.1) from (4.2) we obtain

$$\tfrac{2}{3}t=2\frac{\phi(r)-\phi(s)}{(r+s)^3}-\frac{\phi'(r)-\phi'(s)}{(r+s)^2}. \tag{4.4}$$

The expression on the right-hand side of this equation must remain finite as $r\to r_1$, $s\to -r_1$. But if we write the equation in the form

$$\tfrac{2}{3}t=\frac{2\{\phi(r)-\phi(s)\}-(r+s)\{\phi'(r)-\phi'(s)\}}{(r+s)^3},$$

we see that the right-hand side tends to a finite limit only if $\phi(r)=\phi(-r)$. Hence $\phi(r)$ has to be continued into negative values of r as an even function of r. The function $\phi(r)$ is now defined in the range $-b\leqslant r\leqslant b$, and we assume that all the derivatives which occur are continuous.

Having defined $\phi(r)$ for negative values of r, we can find the position of the face of the cloud at any instant in the first stage of the motion. Equation (4.1) can be written as

$$x-(\tfrac{1}{3}r-\tfrac{2}{3}s)t=\frac{(r+s)\phi'(r)-\phi(r)+\phi(-s)}{(r+s)^2},$$

and the limiting form of this relation as $r\to r_1$, $s\to -r_1$ is easily found by l'Hospital's rule. The result is

$$x_1-2r_1t=\tfrac{1}{2}\phi''(r_1).$$

Similarly, from (4.4) we have

$$t=-\tfrac{1}{4}\phi'''(r_1).$$

Hence the position $x=x_1(t)$ at the face of the cloud is given by

$$x_1=2r_1t+\tfrac{1}{2}\phi''(r_1), \tag{4.5}$$

where r_1 satisfies

$$\phi'''(r_1)=-4t. \tag{4.6}$$

From (4.5) we have

$$\dot{x}_1=2r_1+2\dot{r}_1t+\tfrac{1}{2}\phi'''(r_1)\dot{r}_1=2r_1.$$

But on the face of the cloud c vanishes, and so $2r_1=u(x_1,t)$. Thus the cloud advances into the vacuum with the speed of the gas at the boundary, a result due to McVittie.

There are several points to note about equation (4.5). In the first stage of the motion, r_1 increases continuously from 0 to b. If (4.6) has a solution in this range for positive values of t, it is necessary to assume that $\phi'''(r)<0$ in $0<r<b$, a condition which imposes an additional restriction on the initial data. Again, it may happen that (4.6) has more than one positive root; since $\dot{x}_1=2r_1$, the relevant root is the greatest positive root. Other roots are of no importance; for if a value of r inside the cloud satisfied the relation $\phi'''(r)=-4t$, it would not follow that the corresponding value of s was $-r$.

The inner boundary of the outer layer is fixed by the condition $r=b$. Hence, if we write $x=x_2(t)$, $r=b$, $s=s_2(t)$ in (4.2) and (4.4), we find that this boundary is given by

$$x_2+(\tfrac{1}{3}s_2-\tfrac{2}{3}b)t=\frac{\phi'(s_2)}{b+s_2}+\frac{\phi(b)-\phi(s_2)}{(b+s_2)^2}, \tag{4.7}$$

where *

$$\tfrac{2}{3}t=2\,\frac{\phi(b)-\phi(s_2)}{(b+s_2)^3}-\frac{\phi'(b)-\phi'(s_2)}{(b+s_2)^2}. \tag{4.8}$$

In the region $x_3(t)<x<x_2(t)$, $r=b$; and s is given by

$$\frac{\partial s}{\partial t}-(\tfrac{1}{3}s-\tfrac{2}{3}b)\frac{\partial s}{\partial x}=0,$$

* We note that $s_2=b$ implies $t=0$, thereby verifying our assertion that the inner boundary of the initial non-homogeneous layer splits into two.

which has the solution

$$x+(\tfrac{4}{3}s-\tfrac{2}{3}b)t=g(s).$$

The function $g(s)$ has to be chosen so that s is continuous across $x=x_2$. Comparing this equation with (4.7), we see that

$$x+(\tfrac{4}{3}s-\tfrac{2}{3}b)t=\frac{\phi'(s)}{b+s}+\frac{\phi(b)-\phi(s)}{(b+s)^2}. \tag{4.9}$$

The third moving boundary $x=x_3(t)$ is specified by $s=b$. This gives

$$x_3+\tfrac{2}{3}bt=\frac{\phi'(b)}{2b}.$$

But, by (4.3), $\phi'(b)=0$, and so $x_3=-\tfrac{2}{3}bt$. This boundary has velocity $\dot{x}_3=-\tfrac{2}{3}b=-a$, where a is the velocity of sound in the gas at rest.

5. *The second stage of the motion.*—The motion described in Section 4 will persist so long as the three boundaries are distinct. But if the two boundaries $x=x_1(t)$ and $x=x_2(t)$ coincided at an instant T, at that instant we should have a moving layer $x_3(T)<x<x_1(T)$ in which r is constant; and we could take the state at the instant T as a new initial state. In the subsequent motion, r would remain constant everywhere.

Since $r+s=0$ on $x=x_1(t)$ and $r=b$ on $x=x_2(t)$, the two boundaries would coincide at the instant $t=T$ only if (4.6) and (4.8) gave the same value of T and (4.5) and (4.7) equal values of $x_1(T)$ and $x_2(T)$ when $r_1=b$, $s_2=-b$. This is, in fact, the case; the values are

$$T=-\tfrac{1}{4}\phi'''(b),$$

$$x_1(T)=x_2(T)=2bT+\tfrac{1}{2}\phi''(b).$$

Moreover, at this instant, the two coinciding boundaries have the same velocity $2b=3a$.

When $t>T$, r will be constant everywhere, and s will be given by an equation

$$x+(\tfrac{4}{3}s-\tfrac{2}{3}b)t=g(s)$$

in the moving part of the gas. The function $g(s)$ has to be chosen to fit the conditions at the instant T, and must therefore be the same function as in (4.9). Hence, when $t>T$, the motion is confined to a layer $x_3(t)<x<x_1(t)$ and is specified by

$$r=b,$$

$$x+(\tfrac{4}{3}s-\tfrac{2}{3}b)t=\frac{\phi'(s)}{b+s}+\frac{\phi(b)-\phi(s)}{(b+s)^2}. \tag{5.1}$$

The boundary $x=x_3(t)$, corresponding to $s=b$, is given by $x_3=-\tfrac{2}{3}bt$ as before. The face of the cloud $x=x_1(t)$ is no longer given by (4.5), but is obtained by making $s\to -b$ in (5.1); the result is

$$x_1(t)=2bt+\tfrac{1}{2}\phi''(b). \tag{5.2}$$

Since

$$\dot{x}_1=2b=3a,$$

the face of the cloud advances with a speed equal to three times the velocity of sound in the gas at rest. The model suffers, then, from the same defect as

Burgers' model in respect of this high speed of expansion, but with the important difference that the time T taken to attain this speed can be increased by increasing the depth of the initial layer of non-homogeneity.

6. *A simple example.*—A very simple example is provided by the case when

$$r_0(x) = b\left(1 - \frac{x}{h}\right)^{1/2}.$$

It follows from (4.3) that

$$\phi(r) = hr^2 - \frac{hr^4}{2b^2},$$

when $0 \leqslant r \leqslant b$, no constant of integration being necessary, since it would disappear from (4.1) and (4.2) if it were inserted. As $\phi(r)$ is already an even function, the definition holds in $-b \leqslant r \leqslant b$. It readily follows that the motion in the surface layer is given by

$$x - (r-s)t = h - \frac{h}{b^2}(r^2 - rs + s^2), \tag{6.1}$$

$$r - s = \frac{2b^2t}{3h}. \tag{6.2}$$

At the face of the cloud $x = x_1(t)$, we have $r = -s = r_1(t)$. From (6.2), we have $r_1 = b^2t/3h$, and hence, by (6.1),

$$x_1 = h + \frac{b^2t^2}{3h}.$$

The velocity of the face of the cloud is $\dot{x}_1 = 2b^2t/3h$ in the first stage of the motion, which lasts, as we shall see, until $\dot{x}_1$ attains the value $2b$.

At the inner boundary of the outer layer $x = x_2(t)$, we have $r = b$, $s = s_2(t)$. Hence

$$s_2(t) = b - \frac{2b^2t}{3h}$$

and

$$x_2(t) = \frac{2bt}{3} + \frac{2b^2t^2}{9h}. \tag{6.3}$$

The velocity of the inner boundary is

$$\dot{x}_2(t) = \frac{2b}{3} + \frac{4b^2t}{9h},$$

so that the inner boundary starts to move with the local velocity of sound $2b/3$.

Since

$$x_1 - x_2 = h\left(1 - \frac{bt}{3h}\right)^2,$$

the inner and outer boundaries of the outer layer coincide at the instant $t = 3h/b$. At this instant, $x_1 = x_2 = 4h$, $\dot{x}_1 = \dot{x}_2 = 2b$.

In the region $x_3(t) < x < x_2(t)$, we have $r = b$, and hence

$$x + (\tfrac{4}{3}s - \tfrac{2}{3}b)t = g(s),$$

where $g(s)$ has to be chosen so that $s=s_2$ when $x=x_2$. It is easy to show that

$$x+(\tfrac{4}{3}s-\tfrac{2}{3}b)t=\frac{h(b-s)(b+3s)}{2b^2}. \tag{6.4}$$

But on $x=x_3(t)$, we have $s=b$, and hence

$$x_3=-\tfrac{2}{3}bt,$$

just as in the general case. This completes the description of the first stage of the motion. It lasts until the instant $t=3h/b$; hence the time taken for the outer boundary to attain the velocity $3a$ can be made as long as we please by making h large enough.

In the second stage of the motion, $r=b$; and s is given by

$$x+(\tfrac{4}{3}s-\tfrac{2}{3}b)t=\frac{h(b-s)(b+3s)}{2b^2}.$$

On the face of the cloud we now have $s=-b$, and so

$$x_1=2bt-2h,$$

which advances with constant speed $2b$, whereas on the inner boundary

$$x_3=-\tfrac{2}{3}bt.$$

In conclusion we observe that, if we make $h\to 0$, we find from (6.4) that

$$x+(\tfrac{4}{3}s-\tfrac{2}{3}b)t=0.$$

This is Burgers' solution. We have derived it by considering an initial state, in which the cloud is at rest in $x\leqslant h$, defined by

$$r=s=b\left(1-\frac{x}{h}\right)^{1/2} \qquad (0\leqslant x\leqslant h),$$

$$r=s=b \qquad (x\leqslant 0),$$

and then making h tend to zero. This explains the singularity in the initial state of Burgers' solution to which McVittie refers.

University College, Dundee,
University of St. Andrews:
1950 *February* 16.

THE CONTINUOUS RADIATIVE ABSORPTION CROSS-SECTION OF SINGLY IONIZED POTASSIUM

M. J. Seaton

(Communicated by H. S. W. Massey)

(Received 1950 March 23)

Summary

After obtaining exchange wave functions of K III the continuous absorption cross-section of K II is calculated over the energy range 0 to 13·53 e.V. of the ejected electron, using both the dipole length and the dipole velocity formulae and allowing for the effect of electron exchange. The recommended mean value is taken to be $\alpha_\nu = 3{\cdot}2 \times 10^{-17} \nu_1/\nu$ cm.^{2}, where ν_1 is the frequency at the spectral head.

The cross-section data are used to evaluate the "modified dilution factor" introduced by Strömgren in considering the ionization balance in interstellar space. The possibility of captures to excited states introduces a correction factor of 430 ($T_e = 10^2$), 290 ($T_e = 10^3$), 160 ($T_e = 10^4$), where T_e is the electron temperature (deg. K.). The abundance of interstellar potassium is briefly discussed.

I. *Introduction*

While the quantal theory of continuous radiative absorption cross-sections has been applied to a fair number of neutral atoms, comparatively little work has been done on positive ions.* Singly ionized potassium is a case of some interest as representative of a group of positive ions with outer p^x shells which should be amenable to comparatively accurate calculations. It is also of importance in the study of the ionization balance in interstellar space. The continuous absorption cross-section of K I defies accurate calculation due to great sensitivity to details of the wave functions, and it is therefore fortunate that experimental results are available for this case, enabling a calculation of potassium abundances to be made for H I regions.† For the extension of these calculations to H II regions it is necessary to have data on the absorption cross-section of K II.

II. *The Absorption Cross-section*

(1) *Quantal Formulae for the Cross-section.*—After substituting for the fundamental constants involved, the quantal formula for the continuous absorption cross-section ‡ may be put in the form

$$a_\nu = 8{\cdot}5_5 \times 10^{-19} (I+\epsilon) \mathscr{C}_p \{C_{l-1}\, \sigma^2_{l-1} + C_{l+1}\, \sigma^2_{l+1}\} \text{ cm.}^2, \qquad (1)$$

where the ionization potential I and the energy of ejection ϵ are both expressed in Hartree atomic units (13·53 e.V.). $\mathscr{C}_p$, a factor allowing for the distortion of the wave functions of the passive electrons, is given by

$$\mathscr{C}_p = \prod_{nl \text{ (all passive electrons)}} \left| \int_0^\infty P^i(nl|r) P^f(nl|r)\, dv \right|^2, \qquad (2)$$

* For a general review see D. R. Bates, *M.N.*, **106**, 432, 1946. References to later work are given by D. R. Bates and M. J. Seaton, *M.N.*, **109**, 698, 1949.

† For the experimental results for K I see R. W. Ditchburn, J. Tunstead and J. G. Yates, *Proc. Roy. Soc.* A, **181**, 386, 1943, and for a theoretical discussion, D. R. Bates, *Proc. Roy. Soc.* A, **188**, 350, 1946.

‡ D. R. Bates (1946).

where $P^i(nl|r)/r$ and $P^f(nl|r)/r$ are the radial wave functions, normalized to unity, of the passive electrons in the initial and final states. The factors C_{l-1} and C_{l+1}, which have been tabulated by Bates (1946), arise in averaging over the initial state, summing over the final state, and integrating over the angular coordinates. The fundamental matrix elements, $\sigma_{l\pm1}$, can be expressed in terms of the dipole length ($\sigma_{l\pm1}(L)$) or in terms of the dipole velocity* ($\sigma_{l\pm1}(V)$). In the former case we have

$$\sigma_{l\pm1}(L) = \int_0^\infty P^i(nl|r)P^f(\epsilon, l\pm1|r)\,r\,dr \qquad (3)$$

and in the latter

$$\sigma_{l\pm1}(V) = \frac{2}{I+\epsilon}\int_0^\infty P^i(nl|r)\left\{\frac{2l+1\pm1}{2r}P^f(\epsilon, l\pm1|r) \pm \frac{d}{dr}P^f(\epsilon, l\pm1|r)\right\}dr, \qquad (4)$$

where $P^i(nl|r)/r$ and $P^f(\epsilon, l\pm1|r)/r$ are the radial wave functions of the active electron in the initial and final states, $P^i(nl|r)$ being normalized to unity and $P^f(\epsilon, l\pm1|r)$ to asymptotic amplitude $1/\epsilon^{1/4}$. As remarked by Bates and Seaton (1949) the two expressions for the matrix elements can only be expected to give identical results if the wave functions are solutions of the Schrödinger equation, while the wave functions with which we are concerned are the best separable wave functions for the determination of the energy.

(2) *Hartree-Fock Wave Functions of* KIII.—The equations satisfied by the free electron wave functions of KII involve the wave functions of the KIII core. Although wave functions were available with and without exchange for KII†, none appears to be available for KIII. However, wave functions (without exchange) have been calculated for the iso-electronic case of Cl^- and Cl.‡ Hartree, Kronig and Petersen have remarked that for these the inner part of the charge distribution remains almost unaffected in going from Cl^- to Cl (due to the simultaneous diminution and contraction of the total charge cloud). Thus the tabulated functions $P(1s)$, $P(2s)$ and $P(2p)$ are identical for Cl and Cl^-. An estimate of the wave functions of KIII was therefore made in the following manner :—

(i) $P(1s)$, $P(2s)$ and $P(2p)$ of KIII were taken to be the same as for KII.

(ii) For $P(3s)$ the function $p = P(3s|Cl) - P(3s|Cl^-)$, which is nowhere greater than 0·009, was plotted against $\rho = r/r_m$, where r_m is the principal maximum in the chlorine functions. The value of p on the ρ scale of $P(3s|K\text{II})$ was then read off and the function $P(3s|K\text{III}) = P(3s|K\text{II}) + p$ was calculated and normalized as the required estimate.

(iii) It was not possible to use the same procedure for the $P(3p)$ functions, since $P(3p|Cl^-)$ is much too diffuse with exchange neglected (*cf.* Hartree, 1938). The procedure adopted was to calculate $p = P(3p|Cl) - P(3p|Cl^-)$ as a function of ρ and then to put

$$p' = p \cdot \frac{P(3p|K\text{II})}{P(3p|Cl^-)},$$

---

* S. Chandrasekhar, *Ap. J.*, **100**, 176, 1944; **102**, 223 and 395, 1945. S. Chandrasekhar and F. H. Breen, *Ap. J.*, **104**, 430, 1946.

† D. R. and W. Hartree, *Proc. Roy. Soc.* A, **166**, 450, 1938; and D. R. Hartree, *Proc. Roy. Soc.* A, **143**, 506, 1934.

‡ D. R. Hartree, *Proc. Roy. Soc.* A, **141**, 282, 1933; and D. R. Hartree, R. de L. Kronig and H. Petersen, *Physica*, **1**, 895, 1934.

so that p' tends to zero as $P(3p|K\,\mathrm{II})$ tends to zero. The function

$$P(3p|K\,\mathrm{III}) = P(3p|K\,\mathrm{II}) + p'$$

was calculated and normalized as the required estimate.

The above estimates of the $1s$, $2s$, $2p$ and $3s$ functions were used without further improvement. The estimate of $P(3p|K\,\mathrm{III})$ was used as a first approximation in the solution of the Hartree-Fock equations for $K\,\mathrm{III}$. The final wave function obtained, which is given in Table I, was found to be quite close to the original estimate (nowhere differing from it by more than 0·007).

TABLE I

$P(3p)$ for K III, with exchange

$\epsilon_{3p3p} = 3{\cdot}43$ A.U.

$$\left.\frac{P(3p)}{r^2}\right/_{r=0} = 68{\cdot}9$$

r	$P(3p)$	r	$P(3p)$
0·0	0·000	0·7	−0·582
·01	·006	0·8	− ·735
·02	·023	0·9	− ·839
·03	·047	1·0	− ·898
·04	·076	1·1	− ·923
·05	·108	1·2	− ·919
·06	·142		
		1·4	−0·856
0·08	$0{\cdot}210_5$	1·6	− ·754
·10	$·274_5$	1·8	− ·640
·12	·330	2·0	− ·528
·14	·375	2·2	− ·428
·16	·408	2·4	− ·341
·18	·429	2·6	− ·268
·20	·439	2·8	− ·209
·22	·439	3·0	− ·161
·24	·429	3·2	− ·123
·26	·411	3·4	− ·094
·28	·385	3·6	− ·071
·30	·353	3·8	− ·053
		4·0	− ·040
0·35	0·252		
·40	+ ·131	4·5	$-0{\cdot}018_5$
·45	·000	5·0	− ·008
·50	− ·132	5·5	− ·004
·55	− ·259	6·0	− ·002
·60	− ·378	6·5	− ·001
		7·0	·000

r is in the usual atomic units, $0{\cdot}528_5 \times 10^{-8}$ cm.

As a check on the wave functions the ionization potential of $K\,\mathrm{II}$ was calculated. Neglecting the variation in all wave functions except $P(3p)$, this is given in atomic units by

$$\begin{aligned} I = &[-20F_0(3p3p) + \tfrac{8}{5}F_2(3p3p) - 5\epsilon_{3p3p}]_{K\,\mathrm{III}} \\ &-[-30F_0(3p3p) + \tfrac{12}{5}F_2(3p3p) - 6\epsilon_{3p3p}]_{K\,\mathrm{II}}, \end{aligned} \tag{5}$$

where

$$F_t(nlnl) = \int_0^\infty P^2(nl|r)\frac{1}{r}\left\{\int_0^r P^2(nl|r')\left(\frac{r'}{r}\right)^t dr' + \int_r^\infty P^2(nl|r')\left(\frac{r}{r'}\right)^{t+1} dr'\right\} dr, \tag{6}$$

and the ϵ's are the energy parameters in the Fock equations. The expression for I was found to be very sensitive to the details of the wave function $P(3p)$. The final value obtained, $I=2{\cdot}47$ A.U. was estimated to be correct to within ± 5 per cent so far as the self-consistent procedure is concerned. This is to be compared with the experimental value $I=2{\cdot}341$ A.U.* The experimental value of I was used in all formulae.

The factor $\mathscr{C}_p$ was found to be 0·979.

(3) *Matrix Elements and Cross-section at the Spectral Head.*—The free electron wave functions were calculated at the spectral head from the Hartree-Fock equations using the usual method of successive approximations in which the first approximation is obtained by neglecting the exchange terms. The normalization was carried out by a method due to Strömgren (*cf.* Bates and Seaton, 1949). The matrix elements, calculated using all combinations of exchange and non-exchange wave functions, are given in Table II. We denote a wave function with exchange by P_x and without exchange by P_0. The values shown in ordinary type are obtained from the dipole length formula and those in italic type from the dipole velocity formula. The spectral head cross-section is given in terms of the σ's by

$$a_1=0{\cdot}392(\sigma^2_{l-1}+2\sigma^2_{l+1})10^{-17}\,\text{cm.}^2.$$

TABLE II

$\sigma^2_{l\pm1}$ *for* $\epsilon=0$

	σ^2_{l-1}			σ^2_{l+1}	
	$P_0(\epsilon s)$	$P_x(\epsilon s)$		$P_0(\epsilon d)$	$P_x(\epsilon d)$
$P_0(3p)$	0·48, *0·41*	0·67, *0·34*	$P_0(3p)$	3·8, *2·0*	5·9, *2·3*
$P_x(3p)$	0·29, *0·41*	0·52, *0·38*	$P_x(3p)$	4·0, *2·5*	5·1, *2·5*

It is apparent from Table II that the contribution from $p\rightarrow s$ transitions is much smaller than that from $p\rightarrow d$ transitions. This is a common characteristic of systems with outer p^x shells. The function $P(\epsilon s)$ is small and oscillatory in the region giving the major contribution, while $P(\epsilon d)$ has its first node comparatively far out and rises to a large maximum in the region where $P(3p)$ is large. The exact value of σ^2_{l-1} is of little importance in calculating the cross-section and will not be considered further.

For the d wave it is instructive to compare the position with that of the neutral atoms with outer $2p$ electrons, of which oxygen is a typical example† :

(i) Sensitivity to details of the atomic field.—For oxygen the radial equation for the d wave is so dominated by the term $-6/r^2$ in the region where the potential differs much from its asymptotic form that details of the atomic field are not important. In consequence, there is very little difference between $P_0(\epsilon d)$ and $P_x(\epsilon d)$ and a hydrogenic wave function gives a very good approximation. Due

* J. C. Boyce, *Rev. Mod. Phys.*, **13**, 1, 1941.

† D. R. Bates, *M.N.*, **100**, 25, 1939. Also D. R. Bates and M. J. Seaton (1949).

to the greater nuclear charge the term $-6/r^2$ is not so important for K II and the d wave becomes quite sensitive to details of the atomic field. Exchange appreciably modifies $P(\epsilon d)$, the effect being repulsive, and the hydrogenic approximation is rather poor.

(ii) Cancellation effects.—For oxygen the initial node of $P(\epsilon d)$ is so far out ($r = 9{\cdot}7$ A.U.) that no significant cancellation occurs in the integral for the matrix element. The initial node of $P(\epsilon d)$ for K II occurs at much smaller radial distances ($r = 3{\cdot}6$ without exchange, $r = 4{\cdot}5$ with exchange) but it is still sufficiently far out to exclude any serious cancellation effects.* The contraction is mainly due to the fact that we are now dealing with a positive ion and only to a lesser extent due to the increased nuclear charge.

(iii) Sensitivity to details of the bound electron wave function.—The sensitivity of σ^2_{l+1} to exchange in $P(3p)$ is surprisingly small. This is due to the comparative compactness of the integrand, a significant contribution coming from both sides of the radial distance at which $P_0(3p)$ and $P_x(3p)$ cross over.

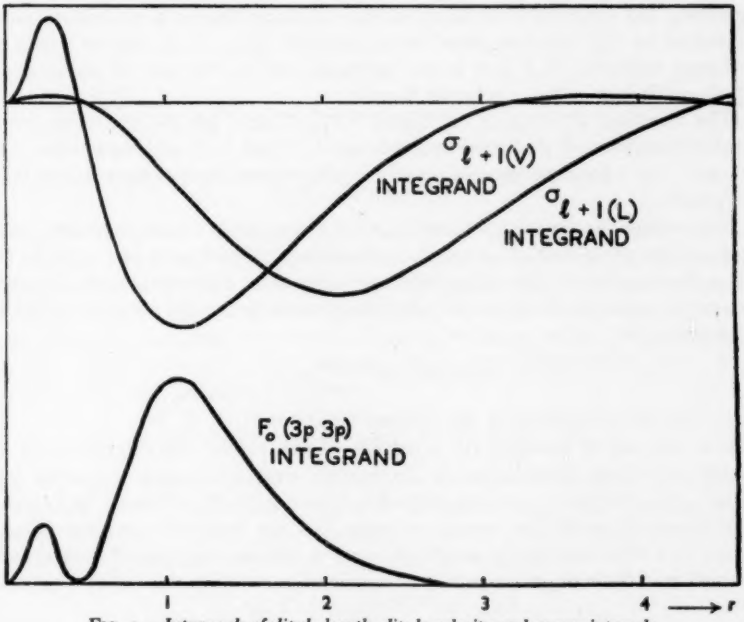

FIG. 1.—*Integrands of dipole length, dipole velocity and energy integrals.*

There is a marked discrepancy between the dipole length and the dipole velocity formulae †, and it is of some importance to decide which is likely to be the more accurate. In Fig. 1 we have plotted the integrands of $\sigma_{l+1}(L)$ and

* A convenient measure of the degree of cancellation in the integral is given by the quantity $(1-D)$, where D is the ratio of the smaller to the larger of the contributions of opposite sign. For $p \rightarrow d$ transitions $(1-D)$ is in all cases greater than 0·8. For comparison we note that Bates found $(1-D)$ for K I ($s \rightarrow p$ transition) to range from 0·388 to 0·015 according to the approximation used. For oxygen, on the other hand, $(1-D)$ is never appreciably below unity for $p \rightarrow d$ transitions.

† That this is a good deal greater than in the case of oxygen is not unexpected in view of the greater complexity of the system.

$\sigma_{l+1}(V)$ and also the integrand of a typical energy integral, $F_0(3p3p)$ (*cf.* equation (6)). It will be noted that the dipole velocity integrand is large in the same regions as the energy integrand, whereas that of the dipole length is still large for radial distances where there is a negligible contribution to the energy. Bearing in mind the principle on which the wave functions are calculated, this would certainly suggest that greater reliance is to be given to the dipole velocity integral, and the smaller sensitivity to details of the wave functions would appear to substantiate this view. It does not, however, seem possible to reach any final decision on this point until a comparison of theory and experiment can be made for at least certain representative substances.* In the meantime the wisest procedure is probably to take a simple mean in order to reduce the maximum possible error. This gives $a_1 = 3{\cdot}2 \times 10^{-17}$ cm.^{2} at the spectral head for the case of full inclusion of exchange.

(4) *Frequency Variation of the Cross-section.*—In order to calculate the frequency variation of a_ν the function $P_x(\epsilon d)$ was calculated for $\epsilon = 0{\cdot}0$, $0{\cdot}2$, $0{\cdot}4$, $0{\cdot}6$, $0{\cdot}8$ and $1{\cdot}0$ A.U. The numerical work was considerably reduced by neglecting the frequency variation of the exchange terms, a procedure which is justified by the fact that these terms are only large in the region where the frequency variation of $P_x(\epsilon d)$ is not excessive and by the lack of sensitivity of $P_x(\epsilon d)$ to details of the exchange terms.

The function $P_x(\epsilon s)$ was calculated for $\epsilon = 0$ and for $\epsilon = 1{\cdot}0$. The corresponding values of $\sigma^2_{l-1}(L)$ were found to be $0{\cdot}52$ and $0{\cdot}46$ and those of $\sigma^2_{l-1}(V)$, $0{\cdot}38$ and $0{\cdot}13$. Intermediate values of σ^2_{l-1} were calculated using a simple linear interpolation.

Fig. 2 gives the frequency variation of a_ν using the two basic formulae. The dipole length cross-section is found to be closely proportional to $1/\nu$ while that of the dipole velocity falls off a little more rapidly. Consistent with the mean value at the spectral head we will take the cross-section to be given as a function of frequency by

$$a_\nu = 3{\cdot}2 \times 10^{-17} \frac{\nu_1}{\nu} \text{ cm.}^2, \tag{7}$$

where ν_1 is the frequency at the spectral head.

It is not easy to estimate the reliability of this result. On the one hand, the absence of serious cancellation in the matrix elements makes any gross error unlikely. On the other hand, the difference between the dipole length and velocity formulae would make one hesitate to assert that the final recommended value is correct to within less than a factor of two. It will be seen that the uncertainty involved is of little importance for the application to the problems of interstellar matter.

III. *Astrophysical Application*

(1) *Interstellar Ionization Equilibrium.*—The analysis of interstellar absorption lines can usually only be expected to give the abundance of an element in a particular stage of ionization; in order to calculate chemical abundances it is

* There is some indirect evidence available on this point. D. R. Bates and A. Damgaard (*Phil. Trans. Roy. Soc.* A, **242**, 101, 1949) consider that it seems likely that the velocity formula gives a better value for the oscillator strengths of spectral lines for complex systems. However, for bound-bound transitions the integrals are necessarily more compact and the problem would not appear to be so acute. (It is of interest to note that Bates and Damgaard find that exchange gives a considerable improvement.) Neon would appear to offer the best possibilities for a direct comparison of theory and experiment.

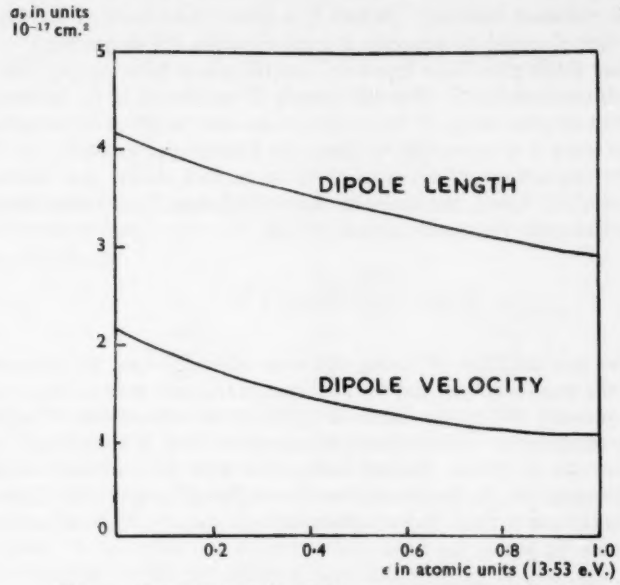

FIG. 2.—*Frequency variation of the cross-section using the dipole length and dipole velocity formulae.*

necessary to study the ionization equilibrium which is set up. In doing this we must bear in mind that the conditions are about as far from thermodynamic equilibrium as it is possible to imagine *, and in particular we cannot expect the principle of detailed balancing to be applicable. Strömgren † has shown that the correct procedure is to equate the rate of photo-ionization from the ground state of an atom or ion to the sum of the recombination rates to all excited states. This procedure gives the ionization equation

$$\frac{\mathscr{R}_1'' \mathscr{R}_e}{\mathscr{R}_1'} = \left(\frac{2\pi m k T_i}{h^2}\right)^{3/2} \cdot \frac{2q_1''}{q_1'} \cdot e^{-I/kT_i} \left(\frac{T_e}{T_i}\right)^{1/2} W, \tag{8}$$

where $\mathscr{R}_e$ is the electron density, $\mathscr{R}_1'$, $\mathscr{R}_1''$ the densities of atoms or ions in the ground state in two consecutive stages of ionization, q_1', q_1'' the corresponding statistical weights. T_i is the radiation temperature, T_e the electron temperature and I the first ionization potential. The factor W is given by

$$W = \frac{q_1' \int_0^\infty \nu^2 a_\nu^1 G_\nu e^{-E_e/kT_i} d\left(\frac{E_e}{kT_i}\right)}{\sum_k q_k' \int_0^\infty \nu^2 a_\nu^k e^{-E_e/kT_e} d\left(\frac{E_e}{kT_e}\right)}, \tag{9}$$

where a_ν^k is the absorption cross-section for the kth excited state of the atom or ion concerned (weight function q_k'), $k = 1$ corresponding to the ground state. E_e is the kinetic energy of the electrons and G_ν is a factor defined by

$$I_\nu = G_\nu \frac{2h\nu^3}{c^2} e^{-h\nu/kT_i}, \tag{10}$$

* *Cf.* A. S. Eddington, *Internal Constitution of the Stars*, Cambridge, 1930.
† Bengt Strömgren, *Ap. J.*, **108**, 242, 1948.

where I_ν is the radiation intensity. (When I_ν is given, the choice of T_i is quite arbitrary; in fact T_i could be eliminated from equation (8) altogether.)

The familiar Eddington-Saha equation has the same form as (8) with W replaced by a dilution factor G. For this reason W is referred to by Strömgren as the " modified dilution factor ". In order to calculate the effect of recombinations to excited states it is convenient to adopt the following procedure. We first calculate W by neglecting all recombinations to excited states, and assuming that a_ν^1 varies as $1/\nu^2$. Using the intensity data of Dunham *, as recommended by Strömgren, this gives for the ionization of K II

$$W(1) = \frac{e^{I/kT_i}}{kT_i} 2{\cdot}87 \times 10^{-33}. \tag{11}$$

Secondly we may calculate W, using the same intensity data, the calculated expression for the cross-sections, and the inclusion of the sum over excited states. Calling this quantity $W(2)$ the ratio $W(1)/W(2)$ is termed the " capture correction " by Strömgren. It has been calculated for *Na* I, *K* I, *Ca* I and *Ca* II and varies from 2·6 to 1600. In calculating the sum over excited states a hydrogenic approximation for the absorption cross-sections, as given by Kramers' formula for *He* II, was judged to be sufficiently accurate.† The denominator of $W(2)$ may then be put in the form

$$q_1' \int_0^\infty \nu^2 a_\nu^1 e^{-E_e/kT_e} d(E_e/kT_e) + 6 \sum_{He\,II} q_k' \int_0^\infty \nu^2 a_\nu^k e^{-E_e/kT_e} d(E_e/kT_e),$$

where the *He* II sum is taken over the $3d$ electron and all n equal to or greater than 4. After the first few terms it is legitimate to replace the *He* II sum by an integral which may be evaluated analytically. Putting $x_n = \dfrac{h\nu_n}{kT_e}$, where ν_n is the spectral head frequency of the nth excited state, we have for the higher excited states of *He* II

$$\sum_{n=n'}^{\infty} q_n' \int_0^\infty \nu^2 a_\nu^n e^{-E_e/kT_e} d(E_e/kT_e)$$

$$= a_1 \nu_1^2 \int_0^{x_{n'}} e^{x_n} \left(\int_{x_n}^\infty \frac{e^{-x}}{x}\, dx \right) dx_n = a_1 \nu_1^2 \left\{ e^{x_{n'}} \int_{x_{n'}}^\infty \frac{e^{-x}}{x}\, dx + \log_e x_{n'} + \gamma \right\},$$

γ being Euler's constant (0·5772). The *He* II sum for $n \geqslant 4$ is given in Table III. It is found that the higher excited states, for which the cross-sections of K II and *He* II would not be far different, give a very considerable contribution to the sum, which justifies using this approximation.

* Theodore Dunham, Jr., *Proc. Amer. Phil. Soc.*, **81**, 277, 1939. The ionization potential of K II being 31·67 e.V. it will be realized that a very considerable extrapolation of black-body intensities has been made in using Dunham's data. Further work on the ultra-violet spectrum of hot stars may call for a revision in the value of the quantity $W(1)$ (equation (11)), but the ratio $W(1)/W(2)$ is not likely to be greatly affected.

† See D. R. Bates, R. A. Buckingham, H. S. W. Massey and J. J. Unwin, *Proc. Roy. Soc.* A, **170**, 322, 1939, for a discussion of this approximation. For the Kramers formula, *cf.* D. R. Bates (1946). The correction factor g was taken to be unity.

TABLE III

T_e	$\sum_{n=4}^{\infty} q_n' \int_0^{\infty} \nu^3 a_\nu^n \exp(-E_e/kT_e) d(E_e/kT_e)$ for *He* II in units $a_1\nu_1^3$ of *He* II
10^3	$2{\cdot}3_2$
10^3	$4{\cdot}5_4$
10^4	$6{\cdot}8_6$

In Table IV we give the "capture correction" for KII, $W(1)/W(2)$, for electron temperature 10^2, 10^3 and 10^4 deg. K., together with the corrected ratio $\mathscr{R}_{K\,III}\mathscr{R}_e/\mathscr{R}_{K\,II}$.

TABLE IV

T_e	$W(1)/W(2)$	$\mathscr{R}_{K\,III}\mathscr{R}_e/\mathscr{R}_{K\,II}$
10^2	430	0·014
10^3	290	0·066
10^4	160	0·38

(2) *Potassium Abundances.*—Since for HI regions we can assume a complete cut-off of radiation beyond the ionization potential of hydrogen the ionization of KII is only of importance in HII regions, where we expect the electron density to be high ($\mathscr{R}_e = \mathscr{R}_H$). From the values of the ratio $\mathscr{R}_{K\,III}\mathscr{R}_e/\mathscr{R}_{K\,II}$ given in Table IV we can see that so long as $\mathscr{R}_e$ is greater than 1 per cm.^{3} the ionization of KII will not be important.

Strömgren (1948) has made a very full analysis of abundances as derived from the absorption lines in χ^2 Orionis, treating separately the hypotheses that the absorbing cloud is an HI region and that it is an HII region. Using the present ionization data we may complete his calculations for potassium. The results are given in Table V.

TABLE V

	H II region	$T_e = 10^4$
$\mathscr{R}_e$	$\mathscr{R}_K$	$\mathscr{R}_K/\mathscr{R}_{Na}$
10	7×10^{-7}	0·06
1	9×10^{-6}	0·08
0·1	30×10^{-5}	0·30

It is interesting to note that for all assumed conditions (except an HII region of low density, which appears to be improbable) the abundance ratio $\mathscr{R}_K/\mathscr{R}_{Na}$ is close to 0·06 for both HI and HII regions.* This is due to the similar mechanism involved if ionization of KII be neglected, since ionization of *Na* II (ionization potential = 47·2 volts) is certainly unlikely to occur.

Acknowledgments

The author wishes to express his thanks to Mr D. R. Bates for his advice and guidance throughout the whole course of this work, and to Professor B. Strömgren for suggesting the problem and for helpful discussions on the astrophysical application. Thanks are also due to the Ministry of Education for the award of a grant.

Department of Mathematics,
University College, London :
1950 *March* 21.

* A summary of work on cosmic abundances is given by R. v. d. R. Woolley and C. W. Allen, *M.N.*, **108**, 292, 1948. The mean value of the ratio $\mathscr{R}_K/\mathscr{R}_{Na}$ is there taken to be 0·13.

VENUS AND THE EARTH'S INNER CORE

K. E. Bullen

(Received 1950 February 22)

Summary

On the hypothesis that the density changes inside the Earth, down to a depth of 5000 km., are essentially due to pressure and conform to the writer's compressibility-pressure Earth model, it is shown that, if Venus and the Earth are of the same primitive composition, it is more probable than not that Venus contains an inner core. This supports the evidence previously found (on the same hypothesis) from the case of Mars that the Earth's inner core is chemically distinct from the rest of the Earth. A formal relation between the rotation period and the ellipticity of Venus is derived and discussed.

1. The use of the Earth model * (Model B) based on a compressibility-pressure hypothesis leads to the suggestion † that Mars may have an inner core, and it therefore becomes desirable to re-examine the constitution of Venus on the basis of Model B. The notation in the present paper will be that of Papers I and III ‡; M and R will here denote the mass and radius of Venus.

2. If Venus has an inner core in the same proportion by mass as in the Earth, the mass of this core, determined in the same way as for Mars (Paper III, Section 4), is $1{\cdot}26 \times 10^{27}$ gm. The mean density of an inner core in Venus can be estimated as in the case of Mars, using the equation (38) of Paper II. As a first approximation, the mean pressure in this core was taken as $2{\cdot}5 \times 10^{12}$ dynes/cm.^{2}, leading to an estimated mean density of 14·7 gm./cm.^{3}. The corresponding first approximation to the radius of the inner core of Venus was 1270 km.

Applying the density-pressure figures in Table III of Paper II to Venus, and taking the crustal layers as in Paper I to be equivalent to a single layer of thickness 30 km. and density 2·8 gm./cm.^{3}, it is found that on the data

(i) $M = 4{\cdot}88 \times 10^{27}$ gm.; $R = 6200$ km.,

(ii) $M = 4{\cdot}88 \times 10^{27}$ gm.; $R = 6300$ km.,

the mass inside a sphere of radius 1270 km. in Venus is $0{\cdot}178 \times 10^{27}$, $0{\cdot}100 \times 10^{27}$ gm., respectively; the corresponding mean densities are 20·4, 11·8 gm./cm.^{3}.

Interpolating linearly, we find that the data

(iii) $M = 4{\cdot}88 \times 10^{27}$ gm.; $R = 6267$ km.

are consistent with the presence of an inner core in Venus of mean density 14·7 gm./cm.^{3} and radius 1270 km. Also, the data

(iv) $M = 4{\cdot}88 \times 10^{27}$ gm.; $R = 6312$ km.

* *M.N., Geophys. Suppl.*, **6**, 50, 1950; this paper will be subsequently referred to as Paper II.
† *M.N.*, **109**, 688, 1950; this paper will be subsequently referred to as Paper III.
‡ *M.N.*, **109**, 457, 1949.

are found to be consistent with the absence of an inner core in Venus. Thus (iii) and (iv) are consistent with an identical primitive composition for Venus and the Earth, assuming Model B to be relevant to the Earth and that the density change at the outer boundary of the central core is due solely to pressure; (iii) assumes that the Earth's inner core is composed of chemically distinct material, while (iv) assumes that the Earth's inner core is due to the prevailing pressure.

The figures (i) are the most probable values of M and R given by the astronomical observations; the estimated standard error of M is $0{\cdot}03 \times 10^{27}$ gm., and of R, 50 km. Thus the data (iii) are practically within the standard errors of the observations, while (iv) are somewhat farther away. Thus, as in the case of Mars, if the Earth Model B is relevant, it is more probable than not that Venus has an inner core. As shown in Paper I, the use of the Earth Model A *, without assuming an inner core, is consistent with the data

$$M = 4{\cdot}88 \times 10^{27}\,\text{gm.};\quad R = 6285\,\text{km.},$$

which are not seriously different from (iii). But the case of Mars makes a sharp discrimination favouring Model B against Model A, if the terrestrial planets are of uniform primitive composition.

Thus the new calculation for Venus gives some small additional support to the view that the terrestrial planets contain inner cores chemically distinct from the remaining materials.

The suggestion made in Paper I on the desirability of improved precision in observations of the diameter of Venus is still very relevant. If the uncertainty could be narrowed to the order of that for Mars, it would be possible, on the theories we have been following, to discriminate much more sharply between various competing Earth models.

3. In Tables I and II the density and pressure distributions in Venus are shown on the hypotheses that the Earth Model B is relevant, and that Venus has not and has an inner core, respectively. In preparing Table II, a second approximation has been made from the figures in the first paragraph of Section 2, resulting in a reduction of 0·6 gm./cm.^{3} in the mean density of the Venus inner core and an increase in the mean radius to 1330 km. The value 6267 km. for R is not sensibly affected in the second approximation. It is likely that if Venus has an inner core, there would be a transition layer corresponding to the layer F in the Earth, and this would have a slight effect on the density distribution in Venus. In view of the limited knowledge concerning the region F, it seems best to ignore this region for the present in constructing Table II; also the extent of density increase inside the inner core is fairly uncertain. On the other hand, Table I, which is not complicated by an inner core, is not subject to these particular uncertainties.

4. The values of I/MR^2 yielded for Venus using (i) the Earth Model A, assuming that Venus has no inner core, (ii) the Earth Model A, assuming that Venus has an inner core, (iii) the density distribution of Table I, (iv) the density distribution of Table II, are 0·360, 0·354, 0·368, 0·362, respectively.

If e is the ellipticity of Venus, and m the ratio of the centrifugal force at the equator to the gravitational attraction, the corresponding values of e/m given on the Radau-Darwin hydrostatic theory are 0·172, 0·168, 0·177, 0·173, respectively.

* K. E. Bullen, *Theory of Seismology*, Cambridge, 1947, p. 218.

TABLE I

d	r	ρ	p
30 km.	6282 km.	3·32 gm./cm.^{3}	0·007 × 10^{12} dynes/cm.^{2}
97	6215	3·36	0·025
97	6215	3·87	0·025
400	5912	4·06	0·150
800	5512	4·25	0·280
1200	5112	4·43	0·41
1600	4712	4·59	0·54
2000	4312	4·74	0·67
2400	3912	4·87	0·79
2800	3512	4·99	0·91
3200	3112	5·11	1·04
3600	2712	5·21	1·15
4000	2312	5·32	1·25
4236	2076	5·57	1·33
4236	2076	9·74	1·33
4400	1912	9·90	1·43
4800	1512	10·18	1·63
5200	1112	10·38	1·78
5600	712	10·54	1·90
6312	0	10·63	1·97

TABLE II

d	r	ρ	p
30 km.	6237 km.	3·32 gm./cm.^{3}	0·007 × 10^{12} dynes/cm.^{2}
95	6172	3·36	0·025
95	6172	3·87	0·025
400	5867	4·02	0·123
800	5467	4·22	0·255
1200	5067	4·40	0·39
1600	4667	4·57	0·52
2000	4267	4·72	0·66
2400	3867	4·86	0·79
2800	3467	5·00	0·92
3200	3067	5·12	1·05
3600	2667	5·25	1·19
4020	2247	5·57	1·33
4020	2247	9·74	1·33
4400	1867	10·13	1·58
4800	1467	10·45	1·84
4937	1330	10·55	1·91
4937	1330	13·3	1·91
6267	0	15·3	2·5

Let the period of rotation of Venus be $20y$ days. Then

$$e = \frac{e}{m} \times \frac{R^3\Omega^2}{\gamma M}, \tag{1}$$

where $\Omega = 3{\cdot}64 \times 10^{-6}y^{-1}$ radians/sec. We shall take $R = 6200 \pm 100$ km., $M = (4{\cdot}88 \pm 0{\cdot}03) \times 10^{27}$ gm., $e/m = 0{\cdot}172 \pm 0{\cdot}005$. Substituting in (1), we have a formula connecting e with y, namely

$$e = (1{\cdot}68 \pm 0{\cdot}07) \times 10^{-6}y^{-2}. \tag{2}$$

The formula (2) could of course be significant only if y were much less than unity, which is not probable on present indications of the rotation period of Venus.

If y is of the order of unity, the value of e would not be resolvable by direct observation, and would in any case almost certainly be dwarfed by surface inequalities sustained by the strength of Venus. Thus on present indications observations of the figure of Venus are not likely to be helpful.

5. The presence of a chemically distinct inner core in the Earth, Mars and Venus is now seen to be independently supported by observations of

(*a*) the mass and radius of Mars,

(*b*) the figure of Mars,

(*c*) the mass and radius of Venus,

assuming that Model B fits the Earth. The cautions attaching to the use of Model B have already been stated in Papers II and III, and the same need remains for further tests that will assist in discriminating between Model B and, for example, Ramsey's proposed modification * of Model A, before too definite conclusions can be drawn.

University of Sydney:
1950 *February* 14.

* *M.N.*, **108**, 406, 1948; *M.N., Geophys. Suppl.*, **5**, 409, 1949.

OCCULTATIONS OF STARS BY THE MOON OBSERVED AT THE NIZAMIAH OBSERVATORY, HYDERABAD, DURING THE YEAR 1949

(Communicated by the Director)

(Received 1950 March 8)

TABLE I

No.	Star	Mag.	Phase	Date 1949		U.T. h	m	s	Obs.
1	B.D.−5° 6048	7·4	D	Jan.	5	16	7	6·4	M.G.
2	B.D.−5° 6056	7·7	D	,,	5	16	41	27·0	M.G.
3	88 Pisc	6·2	D	,,	7	17	44	42·0	M.G.
4	B.D.+6° 185	8·3	D	,,	7	18	6	20·5	M.G.
5	B.D.+10° 257	7·4	D	,,	8	13	24	24·3	M.G.
6	268 Arie	6·1	D	,,	8	17	49	57·3	M.G.
7	107 B Auri	6·5	D	,,	12	19	1	21·3	M.G.
8	49 Auri	5·0	D	,,	13	15	51	13·0	M.G.
9	ι Libr	4·7	R	,,	22	22	44	41·8	M.G.
10	B.D.−7° 6036	6·4	D	Feb.	1	14	23	17·7	M.G.
11	δ Arie	4·5	D	,,	6	13	41	43·2	C.H.
12	36 Taur	5·7	D	,,	7	14	36	29·1	C.H.
13	B.D.+26° 775	6·9	D	,,	8	14	16	52·2	C.H.
14	B.D.+27° 1337	6·4	D	,,	10	18	23	55·6	M.G.
15	B.D.+25° 731	7·5	D	Mar.	7	17	41	48·1	M.G.
16	25 Gemi	6·5	D	,,	9	15	28	58·9	M.G.
17	B.D.+26° 1656	6·8	D	,,	10	18	56	57·3	M.G.
18	B.D.+24° 655	9·0	D	April	3	14	18	53·6	C.H.
19	B.D.+25° 1920	7·1	D	,,	7	18	5	45·4	C.H.
20	28 Canc	6·1	D	,,	7	18	56	25·5	C.H.
21	B.D.+20° 2318	6·7	D	,,	8	18	25	50·5	C.H.
22	B.D.+10° 2230	7·0	D	May	7	19	29	45·4	C.H.
23	B.D.−13° 3824	6·7	D	June	7	15	31	24·7	C.H.
24	44 Pisc	6·0	D	Nov.	2	18	32	30·6	M.G.
25	B.D.−25° 14589	7·2	D	,,	24	14	58	56·7	M.G.
26	B.D.−12° 6327	6·8	D	,,	27	13	25	30·0	M.G.
27	B.D.−11° 5912	6·7	D	,,	27	17	35	2·1	M.G.
28	50 Aqar	5·9	D	Dec.	24	14	39	54·4	M.G.
29	B.D.+23° 537	6·8	D	,,	31	20	50	31·7	M.G.
30	B.D.+23° 538	7·1	D	,,	31	21	2	20·4	M.G.

The last column indicates the following observers :
M.G. : Mahomed Ghouse.
C.H. : C. Hanumantha Rao.

The instrument used throughout was the 15-inch Grubb refractor. The corrections to the standard clock were determined from observations with the transit instrument. The reductions were carried out by S. Aravamuthan assisted by C. Hanumantha Rao. No correction was applied to the observed time.

TABLE II

No.	$\sigma'-\sigma$	$\cos(\rho-\chi)$	$\sin(\rho-\chi)$	No.	$\sigma'-\sigma$	$\cos(\rho-\chi)$	$\sin(\rho-\chi)$
	″				″		
1	−2·2	+0·96	+0·28	16	+0·8	+1·00	−0·06
2	−3·5	+0·97	−0·25	17	−1·9	+0·94	+0·34
3	−1·7	+0·94	+0·34	18	−0·1	+0·63	−0·78
4	+0·2	+0·98	−0·19	19	−1·1	+0·61	+0·79
5	−1·5	+0·97	−0·23	20	−2·9	+0·99	+0·17
6	−0·3	+0·99	−0·16	21	−2·4	+0·19	−0·98
7	−1·4	+0·71	+0·71	22	−1·5	+0·77	+0·64
8	−2·8	+0·92	+0·39	23	−2·0	+0·99	−0·12
9	+1·9	−0·91	+0·41	24	−0·9	+0·27	+0·96
10	−1·3	+0·87	+0·48	25	−2·2	+0·78	+0·62
11	−0·3	+0·80	−0·60	26	−1·0	+0·99	−0·16
12	−2·7	+0·52	+0·85	27	−1·1	+0·99	−0·13
13	+0·5	+1·00	−0·08	28	−1·7	+1·00	+0·02
14	−0·8	+0·63	−0·78	29	−0·8	+1·00	+0·09
15	−1·3	+0·88	−0·47	30	−2·2	+0·83	−0·56

The mean places for 1949·0 of the three stars (Nos. 2, 4 and 18) are given in Table III. For star Nos. 2 and 18, proper motions have been applied to the coordinates given in the catalogue in computing the mean place for use in the reduction.

TABLE III

No.	R.A. (1949·0) h m s	Decl. (1949·0) ° ′ ″	Remarks
2	23 46 7·97	− 4 43 9·1	A. G. Strasburg 8146 ; $\mu_\alpha - 0^s{\cdot}0012$; μ_δ 0 (Yale)
4	1 12 53·95	+ 6 41 12·1	Boss 1511
18	4 21 36·79	+25 2 43·7	A. G. Berlin 1421 ; $\mu_\alpha + 0^s{\cdot}0027$; $\mu_\delta - 0''{\cdot}018$

Nizamiah Observatory,
Hyderabad, Deccan, India :
1950 *February* 4.

ERRATUM

M.N., **110,** No. 1, 1950, P. A. Sweet's paper:

P. 76, equations (3.12) and (3.15), and the line immediately following equation (3.15), *for* $\boldsymbol{w}$ *read* $\overline{\boldsymbol{w}}$.

CONTENTS

PAGE

Meeting of 1950 March 10:
Fellows elected 197
Presents announced 197

Meeting of 1950 April 14:
Fellows elected 198
Presents announced 198

Helen W. Dodson and Edwin B. Weston, A study of the eruptive prominence of 1948 September 27 199

R. v. d. R. Woolley and K. Gottlieb, Monochromatic magnitudes observed with a coarse grating 206

Lyman Spitzer, Jr., On the interpretation of measured solar wave-lengths ... 216

J. v. B. Lourens and T. W. Russo, The Cape and Radcliffe observations of the Eclipse Comet (1948 l) 220

G. C. McVittie, The expansion of an interstellar gas-cloud into a vacuum 224

E. T. Copson, The expansion of a gas cloud into a vacuum 238

M. J. Seaton, The continuous radiative absorption cross-section of singly ionized potassium 247

K. E. Bullen, Venus and the Earth's inner core 256

Hyderabad, Nizamiah Observatory, Occultations of stars by the Moon observed at the Nizamiah Observatory, Hyderabad, during the year 1949 260

Erratum 261

Printed in London by Taylor & Francis, Ltd., 1950 October.